

1 **Title:** Fractalkine-induced microglial vasoregulation occurs within the retina and is altered
2 early in diabetic retinopathy

3 **Author affiliations:** *Samuel A. Mills^a, *Andrew I. Jobling^a, *Michael A. Dixon^a, Bang V.
4 Bui^b, Kirstan A. Vessey^a, Joanna A. Phipps^a, Ursula Greferath^a, Gene Venables^a, Vickie H.Y.
5 Wong^b, Connie H.Y. Wong^c, Zheng He^b, Flora Hui^b, James C. Young^a, Josh Tonc^a, Elena
6 Ivanova^d, Botir T. Sagdullaev^d, Erica L. Fletcher^a

7 * Joint first authors

8 ^a Department of Anatomy and Neuroscience. The University of Melbourne, Parkville 3010
9 Victoria, Australia.

10 ^b Department of Optometry and Vision Sciences. The University of Melbourne, Parkville
11 3010 Victoria, Australia.

12 ^c Department of Medicine, Centre for Inflammatory Diseases, School of Clinical Sciences,
13 Monash University, Clayton, Victoria, Australia

14 ^d Burke Neurological Institute at Weill Cornell Medicine, White Plains, New York 10605,
15 USA.

16 **Corresponding author:** Prof. Erica L. Fletcher.

17 Email: elf@unimelb.edu.au

18 **Classification:** Biological Science / Cell biology

19 **Keywords:** retina, microglia, capillary regulation, fractalkine, diabetes

20 **Author Contributions:** E.L.F., A.I.J., B.V.B. and S.A.M. designed the experiments and wrote
21 the manuscript. S.A.M., B.V.B., M.A.D., J.A.P., G.V., V.H.Y.W., C.H.Y.W. and A.I.J.
22 conducted the experiments. U.G., K.A.V., Z.H., E.I., B.T.S., F.H., J.T. and J.C.Y. acquired
23 and analysed data. E.L.F., S.A.M., M.A.D. and A.I.J. are guarantors of this work and have
24 full access to all the data. They take responsibility for the integrity and accuracy of the data.

25 **This pdf includes**

1 Main text

2 Fig. 1-6

3

1 **Abstract**

2 Local blood flow control within the CNS is critical to proper function and is dependent on
3 coordination between neurons, glia and blood vessels. Macrogia such as astrocytes and
4 Müller cells, contribute to this neurovascular unit within the brain and retina, respectively.
5 This study explored the role of microglia, the innate immune cell of the CNS, in retinal
6 vasoregulation and highlights changes during early diabetes. Structurally, microglia were
7 found to contact retinal capillaries and neuronal synapses. In the brain and retinal explants,
8 the addition of fractalkine, the sole ligand for monocyte receptor Cx3cr1, resulted in capillary
9 constriction at regions of microglial contact. This vascular regulation was dependent on
10 microglial involvement, since mice lacking Cx3cr1, exhibited no fractalkine-induced
11 constriction. Analysis of the microglial transcriptome identified several vasoactive genes,
12 including angiotensinogen, a constituent of the renin-angiotensin system (RAS). Subsequent
13 functional analysis showed that RAS blockade via candesartan, abolished microglial-induced
14 capillary constriction. Microglial regulation was explored in a rat streptozotocin (STZ) model
15 of diabetic retinopathy. Retinal blood flow was reduced after 4 weeks due to reduced
16 capillary diameter and this was coincident with increased microglial association. Functional
17 assessment showed loss of microglial-capillary response in STZ-treated animals and
18 transcriptome analysis showed evidence of RAS pathway dysregulation in microglia. While
19 candesartan treatment reversed capillary constriction in STZ-treated animals, blood flow
20 remained decreased likely due to dilation of larger vessels. This work shows microglia
21 actively participate in the neurovascular unit, with aberrant microglial-vascular function
22 possibly contributing to the early vascular compromise during diabetic retinopathy.

23

1 **Significance Statement**

2 This work identifies a novel role for microglia, the innate immune cells of the CNS, in the
3 local control of the retinal vasculature and identifies deficits early in diabetes. Microglia
4 contact neurons and vasculature and express several vasoactive agents. Activation of
5 microglial fractalkine-Cx3cr1 signalling leads to capillary constriction and blocking the
6 renin-angiotensin system (RAS) with candesartan abolishes microglial-mediated
7 vasoconstriction in the retina. In early diabetes, reduced retinal blood flow is coincident with
8 capillary constriction, increased microglial-vessel association, loss of microglial-capillary
9 regulation and altered microglial expression of the RAS pathway. While candesartan restores
10 retinal capillary diameter early in diabetes, targeting of microglial-vascular regulation is
11 required to prevent coincident dilation of large retinal vessels and reduced retinal blood flow.

12

13

1 **Introduction**

2 The retina is one of the most metabolically active organs in the body, and in most mammals
3 is supplied by an outer (choroidal) and inner (retinal) vascular network (1). While the choroid
4 provides for the light-detecting photoreceptors within the outer retina, the retinal blood
5 supply supports the numerous neurons and glia found in the ganglion cell and inner nuclear
6 layers of the retina (2). The arterioles of the retinal blood supply enter at the optic disc and
7 branch to form sequentially smaller vessels, including the retinal capillaries, establishing the
8 superficial vascular plexus. These capillaries penetrate the inner retina, forming the relatively
9 sparse intermediate vascular plexus, and deeper towards the outer retina forming the highly
10 anastomosed deep vascular plexus. Completing the vascular circuit, blood returns via the
11 venules on the retinal surface, which exit alongside the optic nerve (3, 4).

12
13 Blood flow throughout the retina is largely dependent on vessel calibre, which is tightly
14 regulated to meet the metabolic demands of neuronal activity (5). An example of this is the
15 well-defined hyperaemic response, whereby increased neuronal activity (via flickering light)
16 results in arteriole dilation and increased inner retinal blood flow (6). Unlike peripheral blood
17 vessels, retinal and brain vasculature have no direct neuronal input to modulate vascular tone,
18 rather macroglial cells (Müller cells and astrocytes) are thought to actively regulate vascular
19 calibre in response to changes in neural activity (7, 8). This type of coupling has given rise to
20 the idea of a neurovascular unit, encompassing neurons, glia and blood vessels (7). While
21 studies within the retina identified neuronal-dependent calcium increase in Müller cells to
22 mediate vessel diameter change (9), more recent data suggest regulation of the inner retinal
23 vasculature is more complex (10). Evidence for this comes from the fact that the same light
24 stimulus can induce either vasoconstriction or vasodilation, and Müller cell-dependent

1 calcium signalling only controls capillaries within the intermediate vascular plexus (11, 12).

2 This suggests the existence of multiple regulatory pathways within the retina.

3

4 Recently it has been proposed that microglia, the innate immune cells of the retina, may also

5 play a role in the neurovascular unit, although direct functional evidence is lacking (13). The

6 conventional view of microglia is that they contribute to disease via the release of pro-

7 inflammatory and neurotoxic cytokines (14-16). However, it is now recognised that microglia

8 play several important, inflammation-independent roles in the normal brain and retina, such

9 as dynamic synaptic surveillance and synaptic pruning (17-19). Despite this, the

10 inflammation-independent response of microglia to neuronal signalling and their role in the

11 regulation of vascular tone has yet to be confirmed.

12

13 While regulation of retinal blood flow is critical to retinal function (20), vascular dysfunction

14 is known to occur in several pathologies, including diabetic retinopathy (DR). Early in the

15 progression of DR, vascular pathology such as reduced retinal blood flow, micro-aneurysms

16 and areas of vascular non-perfusion occur (21). Reduced retinal blood flow, in particular,

17 presents early in humans with diabetes (22-24), and in animal models of diabetes (24).

18 Altered inner retinal vascular regulation is considered a likely precursor to the development

19 of severe vascular pathology in DR (25).

20

21 The present study investigates whether retinal microglia form a functional component of the

22 neurovascular unit, and whether signalling through the fractalkine-Cx3cr1 pathway

23 modulates vascular diameter. In addition, the work explores whether altered microglial

24 involvement with the inner retinal vasculature may help explain the reduced retinal blood

25 flow that occurs early during diabetes. Exploring the mechanisms responsible for the tight

- 1 regulation between retinal neuronal activity and the local blood supply is critical to
- 2 understanding retinal function in health and disease and may provide an empirical framework
- 3 for future therapies targeting vascular pathogenesis.

1 **Results**

2 **Microglia contact both retinal vasculature and neuronal synapses**

3 Microglia within the CNS have a close association with the vasculature, particularly during
4 injury and disease (26). However, less is known about microglial-vascular interactions in
5 normal tissue. Within the retina, microglial cell bodies typically reside in the plexiform
6 layers, while their processes extend throughout the retina (see *SI appendix*, Fig. S1).
7 Inspection of the superficial vascular plexus shows microglia tiling the whole tissue (Fig. 1A,
8 Cx3cr1^{GFP/+} mouse retina, EGFP, green) and in close association with retinal vasculature
9 (Fig. 1A *inset*; IB4, red). When microglial process contact with retinal vessels of different
10 diameters is quantified relative to the respective area of each vessel diameter class, microglia
11 are seen to interact with smaller retinal vessels ($\leq 15\mu\text{m}$), particularly the smallest retinal
12 capillaries ($< 10\mu\text{m}$), when compared to the larger vessels (Fig. 1B; one-way ANOVA, $p <$
13 0.05 , 0.001 for $15\text{-}20\mu\text{m}$ and $> 20\mu\text{m}$, respectively). At the ultrastructural level (Fig. 1C;
14 Cx3cr1^{GFP/+} mouse retina), a microglial process (MC, stained for EGFP) abuts a pericyte
15 (PC), which lies over an endothelial cell (EC) lining the capillary lumen (CL). This
16 microglial-pericyte contact is also investigated immunohistochemically using the NG2-
17 DsRed reporter mouse, which labels pericyte somata and processes (Fig. 1D, red). A
18 microglial cell (Iba-1, green) is observed to make contact with two pericyte somata (red),
19 with nuclei immunolabelled with DAPI (blue). Orthogonal projections (top and right) from
20 the boxed area, show direct contact between the two cell types. The contact indicated with the
21 asterisk was further imaged at higher resolution to show direct contact between the microglial
22 process (green) and the pericyte soma (red; asterisk in Fig. 1E, also see *SI appendix*, Fig. S2
23 and Video S2). The extent of microglial contact with pericytes somata, processes (NG2-
24 labelled) and capillary areas devoid of pericyte contact (NG2 negative / IB4 positive regions)
25 was quantified in rat retina, with no preference observed for microglial-pericyte or

1 microglial-vessel contact (Fig. 1F). In addition to contacting retinal vessels (IB4, magenta,
2 asterisk in Fig. 1G), microglia (EGFP, green) are also observed to extend processes into the
3 inner plexiform layer (IPL), where neuronal synapses reside (Fig. 1G, VGLUT1 red, arrow
4 heads; DAPI blue). The *inset* shows a rendering of these microglial-neuronal interactions at
5 higher magnification. This is also observed in the human retina (Fig.1H, DAPI, blue) with
6 microglia (Iba-1, green) contacting both retinal vessels (vitronectin, magenta, asterisk) and
7 neuronal synapses (VGLUT1, red. arrow heads). When quantified in the *Cx3cr1^{+GFP}* mouse
8 retinae, the majority of microglia (EGFP, green) in the inner retina contact both neuronal
9 synapses (VGLUT1, blue) and retinal vessels (IB4, red; Fig. 1I inset, $73 \pm 13\%$, rat retina).
10 All individual channels for immunolocalization are shown in *SI appendix* (Fig. S3)

11

12 **Microglia modulate vessel diameter and express vasoactive genes**

13 Within the brain and retina, macroglial (astrocyte and Müller cell) cell contact with neuronal
14 synapses and vasculature is critical for local control of blood supply in response to neuronal
15 activity (7, 8). To determine whether microglia play a similar role, *Cx3cr1^{GFP/+}* retinae were
16 isolated and maintained *ex vivo*. Microglia were visualised via their expression of EGFP (Fig.
17 2A; green) and vessels were labelled with rhodamine B (Fig. 2A; red). As the fractalkine-
18 *Cx3cr1* axis is thought to mediate neuronal-microglial communication, blood vessels and
19 microglia were imaged while fractalkine (200ng/ml) or PBS was perfused into the chamber
20 (*SI appendix*, Video S1). Vessel diameter change was monitored and expressed relative to the
21 baseline value for the same region of vessel.

22

23 In response to fractalkine, blood vessel regions that were associated with microglial processes
24 (m+) constricted (Fig. 2B m+; 2-way ANOVA; PBS versus fractalkine, $p < 0.001$), while
25 those regions that were further away from microglial processes (m-) exhibited no significant

1 alteration in capillary diameter (Fig. 2B m-; 2-way ANOVA; PBS versus fractalkine, $p =$
2 0.26). These *ex vivo* preparations showed minimal microglial process movement at the
3 vascular level throughout the imaging, including during fractalkine exposure (*SI appendix*,
4 Video S1 and Fig. S4). When explants taken from animals lacking Cx3cr1 ($Cx3cr1^{GFP/GFP}$)
5 were exposed to fractalkine, no alteration in vessel diameter was observed compared to PBS
6 controls at regions with (m+; $105.7 \pm 2.7\%$ versus $94.7 \pm 2.3\%$, 2-way ANOVA $p=0.52$) or
7 without (m-; $98.8 \pm 1.2\%$ versus $97 \pm 1.3\%$, 2-way ANOVA $p=0.999$) microglial contact
8 (Fig. 2B). Finally, to explore whether this vasomodulatory function of fractalkine was retina-
9 specific, superficial vessels within the rat brain were imaged using a thin skull preparation.
10 These preliminary data showed that while vehicle delivery resulted in no alteration in vessel
11 diameter, the subdural addition of fractalkine lead to a significant constriction of the smaller
12 vessels (Fig. 2 C; RM 2-way ANOVA, vessels $\leq 15\mu\text{m}$, $p < 0.05$). While both tissues show a
13 fractalkine-induced constriction, the difference in vessel kinetic response likely reflects the
14 different systems used to explore microglial vasoregulation (*ex vivo* and *in vivo*,
15 respectively).

16
17 Since the $Cx3cr1^{GFP/GFP}$ retina showed no fractalkine-induced vessel constriction, microglial
18 contact with retinal vessels and neurons was explored. High resolution immunocytochemical
19 analysis of microglia (EGFP, green) contact with neuronal synapses (VGLUT1, red) and
20 vessels (IB4, light blue) was undertaken to enable specific areas of contact to be quantified
21 (Fig. 2D). When the volume of contact per individual microglia was calculated,
22 $Cx3cr1^{GFP/GFP}$ animals had fewer vessel contacts than animals with one functional copy of
23 Cx3cr1 (Fig. 2E; $Cx3cr1^{GFP/+}$ $7.5 \pm 0.4\%$ versus $Cx3cr1^{GFP/GFP}$ $5.5 \pm 0.3\%$, t -test $p=0.004$).
24 While there was no difference in neuronal contacts between the two genotypes,
25 $Cx3cr1^{GFP/GFP}$ animals showed less microglial process branching (Fig. 2E; $Cx3cr1^{GFP/+}$ 111.5

1 ± 7.2 versus $Cx3cr1^{GFP/GFP}$ 92.2 ± 2.1 , t -test $p=0.03$), reflecting the literature showing
2 $Cx3cr1^{GFP/GFP}$ to have a more activated inflammatory profile (28). When retinal capillary
3 diameters were compared to C57bl6 control animals, $Cx3cr1^{GFP/+}$ capillaries were similar to
4 controls (Fig. 2F; C57bl6 $11.3 \pm 0.3\mu\text{m}$ versus $Cx3cr1^{GFP/+}$ $10.9 \pm 0.2\mu\text{m}$, 1-way ANOVA
5 $p=0.66$), while $Cx3cr1^{GFP/GFP}$ showed increased capillary diameters (Fig. 2F; $Cx3cr1^{GFP/+}$
6 $10.9 \pm 0.2\mu\text{m}$ versus $Cx3cr1^{GFP/GFP}$ $12 \pm 0.4\mu\text{m}$, 1-way ANOVA $p=0.047$). There was no
7 difference in larger vessel diameter for any genotype (Fig. 2F inset; $p=0.87$ and 0.94 for
8 $Cx3cr1^{GFP/+}$ and $Cx3cr1^{GFP/GFP}$, respectively).

9
10 RNA-Seq was performed on FACS-isolated microglia collected from 12-week-old dark
11 agouti rats to determine whether vasomodulatory factors were contained within the microglial
12 transcriptome. To confirm the purity of sample, the mapped genes were compared to a
13 published list of microglial markers (29), with 23/29 markers identified in our gene
14 population, including the microglial-specific marker *Tmem119* (*SI appendix*, Table S1)(41).
15 The microglial transcriptome was also compared to microglial-enriched genes reported in
16 several studies, with significant overlap observed, while there was little contamination from
17 known neuronal genes (*SI appendix*, Fig. S5). The expressed gene population was compared
18 against genes known to be involved in angiogenesis (GO:0001525, 407 genes) and regulation
19 of blood vessel diameter (GO:0097746, 310 genes). In total, 268 genes expressed in the
20 microglial population were identified to have roles in angiogenic pathways (Fig. 2G, and *SI*
21 *appendix*, table S2), such as hypoxia inducible factor 1 alpha (*Hif1a*) and vascular endothelial
22 growth factor A and B (*Vegf A/B*). When vessel diameter regulation was explored, 41 genes
23 were found to have a role in vasodilation such as phospholipase A2 (*Pla2g6*) and sirtuin 1
24 (*Sirt1*), while 39 genes were identified with vasoconstriction, including endothelin 1, 3

1 (*Edn1*, 3) and arachidonate 5-lipoxygenase (*Alox5*) and angiotensinogen (*Agt*; Fig. 2G, and SI
2 appendix, tables S3 and S4, respectively).

3

4 As angiotensinogen is a constituent of the renin-angiotensin system (RAS), which is involved
5 in retinal vessel regulation via the angiotensin II receptor type 1 (AT1R) (30, 31), *ex vivo*
6 experiments were performed using the AT1R antagonist, candesartan. Baseline capillary
7 diameter was averaged over 10 minutes in rat retinal explants exposed to Ames (black trace)
8 and Ames + candesartan (230 nM; red trace) and after which time fractalkine was added
9 (shaded area in Fig. 2H). Similar to that observed in the *Cx3cr1^{GFP/+}* mouse (Fig. 2A, 2B),
10 exposure of the rat retinae to fractalkine induced capillary constriction, while exposure to
11 candesartan blocked any fractalkine-induced constriction (Fig. 2H). When grouped data were
12 analysed, candesartan abolished the fractalkine-induced vasoconstriction (Fig. 2I, *t*-test,
13 $p < 0.01$). To further support the role of RAS in microglial-mediated vessel regulation, control
14 C57bl6 and *Cx3cr1^{GFP/GFP}* were exposed *ex vivo* to fractalkine (FKN) for 2 hours, microglia
15 isolated and the expression of angiotensinogen (*Agt*) quantified (Fig. 2I inset). While
16 exposure to fractalkine increased *Agt* expression in control retinae, *Cx3cr1^{GFP/GFP}* retinae
17 which previously exhibited no microglial-mediated constriction (Fig. 2B), showed no
18 expression change (Fig. 2I inset; +FKN, C57bl6 21.8 ± 3.5 copies/1000 copies *Hprt* versus
19 *Cx3cr1^{GFP/+}* 7.7 ± 0.6 copies/1000 copies *Hprt*, 2-way ANOVA $p = 0.017$). The current data
20 show that microglia are capable of modulating vascular constriction within the retina and
21 broader regions of the CNS via the fractalkine-Cx3cr1 pathway. While they express several
22 gene transcripts for known vasoactive agents, microglial regulation of retinal vessels occurs
23 via AT1R activation.

24

25 **Retinal blood flow and capillary diameter is changed in early diabetes**

1 The regulation of retinal blood supply is critical to normal function, with retinal pathologies,
2 such as DR, exhibiting early retinal blood flow defects and abnormal neurovascular coupling
3 (22, 24, 32). To explore whether microglial vasoregulation was altered during early diabetes,
4 adult dark agouti rats were rendered diabetic via a single injection of STZ with significant
5 hyperglycaemia evident throughout the 4-week experimental period (*SI appendix*, table S5).

6
7 As reduced retinal blood flow is a consistent and early alteration in patients with diabetes and
8 animal models (23, 24), quantitative vessel-dependent kinetic analysis using sodium
9 fluorescein (33) was used to confirm vascular dysfunction. Average normalised fluorescence
10 intensity was calculated over time for every pixel within the fundus image (see Fig. 3A, B, C
11 *insets*), grouped on vessel type, and *en face* heat-maps produced (Fig. 3A, B, C, fill times),
12 with warmer colours indicating greater time taken to fill (slower blood flow). Vessel-
13 dependent kinetic analysis revealed arterioles in STZ-treated animals took longer to fill (Fig.
14 3D; median regression analysis, $p < 0.05$), reflecting reduced blood flow. Due to the serial
15 nature of the retinal vasculature, this increase in fill time was also observed in retinal
16 capillaries and venules (Fig. 3D; median regression analysis, $p < 0.05$), with no vessel-
17 specific deficit identified (median regression analysis, $p > 0.05$). Drain times were also longer
18 in all retinal vessels (Fig. 3E; median regression analysis, $p < 0.05$), with the effect
19 significantly greater than that observed for fill times (median regression analysis, $p < 0.05$).

20 The reduced arteriolar and venular blood flow in STZ-treated animals was verified using
21 velocimetry (*SI appendix*, Fig. S6) and the clinically relevant arterio-venous transit time was
22 also exhibited reduced blood flow (increased transit time, *SI appendix*, Fig. S6D). The
23 decrease in retinal blood flow kinetics was independent of systemic change, with systolic
24 blood pressure, blood haematocrit and intraocular pressure unaltered (*SI appendix*, Fig. S7).

25

1 As vessel change affects blood flow in DR (34, 35), the morphology of large diameter vessels
2 was assessed from fluorescein images at peak fluorescent intensity. No change in retinal large
3 vessel tortuosity (Fig. 3F; 2-way ANOVA, arterioles $p = 0.52$, venules $p = 0.98$), or arteriole
4 / venule diameter (arteriovenous ratio, Fig. 3F inset; t -test, $p = 0.48$) was observed between
5 the two cohorts of animals. Similarly, when arteriole, capillary and venule densities were
6 separately quantified using retinal wholemount immunohistochemistry (Fig. 3G inset shows
7 the rendered image of arterioles, dark blue; venules, cyan; and capillaries, yellow), no change
8 in vessel densities were observed between control and STZ-treated animals (Fig. 3G, 2-way
9 ANOVA, arterioles $p = 0.98$, venules $p = 0.99$, capillaries $p = 0.94$). As fluorescein image
10 analysis and immunohistochemistry lack the resolution to assess capillary diameter, OCTA
11 was used to quantify this *in vivo*. Images of the superficial retinal capillary network were
12 obtained for control (Fig. 3H) and STZ-treated (Fig. 3H inset) animals and quantification
13 (green overlay showing measured capillaries) revealed a decrease in capillary diameter in the
14 STZ-treated cohort (Fig. 3I; 2-way ANOVA, $p < 0.05$). When a similar analysis was
15 performed on the intermediate and deep capillary plexi (I/DVP), no alteration in diameter was
16 detected (Fig. 3I; 2-way ANOVA, $p=0.72$).

17

18 In summary, retinal blood flow was significantly slower in diabetes, with *in vivo* OCTA
19 revealing retinal capillary constriction within the superficial vascular plexus 4 weeks after
20 STZ-induced diabetes. These diameter changes were restricted to the capillary network, as
21 larger vessels remained unaltered and there was no change in retinal vascular coverage.

22

23 **Retinal microglia contact with capillaries and pericytes is increased in early diabetes,**
24 **independent of activation**

1 The extent of microglial (Fig. 4A *inset*, green, Iba-1) contact with arterioles, capillaries and
2 venules (Fig. 4A *inset* red, IB4) was quantified for control and STZ-treated animals to
3 determine whether the retinal capillary constriction in diabetes was accompanied by altered
4 microglial association. While microglia exhibited a similar association with large diameter
5 arterioles and venules (Fig. 4A; 2-way ANOVA, $p > 0.99$ and $p > 0.66$, respectively),
6 microglial-capillary association was increased in STZ-treated animals (Fig.4A; 2-way
7 ANOVA, $p < 0.05$). In addition, microglial-pericyte association (Fig. 4B *inset* microglia
8 green, Iba-1; pericytes light blue, NG2, vessels red, IB4) was increased within the central
9 retina of STZ-treated animals (Fig. 4B, 2-way ANOVA, $p < 0.05$). There was no vessel
10 dropout (Fig. 3G), nor loss of retinal pericytes (*SI appendix*, Fig. S8) at this early stage of
11 diabetes. The association of microglia with pericytes and capillary areas lacking pericyte
12 contact was further explored in control and STZ-treated animals using quantitative image
13 analysis (Fig. 4C *inset*, rendered image showing pericyte somata red; pericyte processes
14 green; pericyte-free vessel blue and skeletonised microglia). While quantitative analysis
15 showed no specific preference for microglia to contact pericyte somata, processes or capillary
16 areas lacking pericytes (Fig.4C; 2-way ANOVA, $p = 0.16$), there was increased microglial
17 association with all three at 4 weeks of diabetes (Fig.4C; 2-way ANOVA, $p < 0.01$). To
18 determine whether this microglial effect was specific, or a result of a more generalised
19 macroglial response as has been shown in later stages of diabetes (36, 37), astrocyte density
20 and Müller cell gliosis were quantified. Vessel-specific astrocyte coverage (Fig 4D) and
21 Müller cell gliosis (Fig. 4E) were unaltered after 4 weeks STZ treatment (2-way ANOVA, p
22 > 0.92 and 0.99 respectively).

23

24 Previous work has shown blood-retinal barrier (BRB) integrity is compromised early in
25 diabetes (38). Using vessel-dependent blood flow analysis (Fig.3A-E), we used the return to

1 baseline after fluorescein peak (fluorescein offset) as a measure of BRB integrity. While no
2 alteration in offset was observed for larger vessels, retinal capillaries showed a significant
3 increase, indicative of fluorescein leakage / reduced BRB integrity (Fig. 4F; median
4 regression analysis, $p < 0.05$). A breakdown in BRB can lead to immune cell infiltration and
5 microglia activation, with microglial migration and morphological change indicative of
6 classical activation observed in the retina, 1 month post-STZ (39). To assess whether altered
7 microglial-vessel association occurred in the context of monocyte involvement / microglial
8 activation, wholemounts were co-labelled with IB4 and Iba-1 and the number and
9 morphology of microglia quantified in central and peripheral retina. Despite the increase in
10 capillary fluorescein offset, there was no difference in the number of monocytes / retinal
11 microglia (Fig. 4G; 2-way ANOVA, central $p = 0.4$, peripheral $p = 0.9$), or microglial
12 morphology after 4 weeks of hyperglycaemia (Fig. 4H; 2-way ANOVA, cell body area $p >$
13 0.99 , process length/cell $p = 0.15$, branch points/cell $p > 0.99$). Despite this, *Cx3cr1*
14 expression was increased in the diabetic retina (*SI appendix*, Fig. S9). RNAseq analysis of
15 microglial isolates from 4-week control and STZ-treated animals showed that of the 254
16 differentially expressed genes, 22 inflammatory response genes were identified, 15 of which
17 were positive regulators (GO: 0050729), while 12 were negative regulators of inflammation
18 (GO: 0050728) (Fig. 4I; *SI appendix*, tables S6 and S7). Importantly, chemokine and
19 cytokines normally associated with microglial activation, including Tlr2, Il-1 β , Cxcl10, TNF-
20 a, IL-1a, C1q were not altered and there was no expression of the infiltrating monocyte
21 marker gene, *Ccr2*, in our RNAseq dataset (40, 41). Thus, at this early stage of diabetes (4-
22 weeks) when retinal capillaries are constricted, there is increased microglial-capillary
23 interaction, which is independent of monocyte recruitment, classical microglial activation and
24 a more generalised macroglial response.

25

1 **Microglial expression of vasoactive genes and control of capillary constriction are**
2 **altered in early diabetes**

3 To determine whether there was a loss of retinal vasomotor control during early diabetes,
4 breathable oxygen was used to induce hyperoxic challenge and capillary diameter within the
5 superficial vascular plexus was quantified using OCTA (Fig. 5A image). While control
6 animals showed a distinct vasoconstriction in response to 100% oxygen, no constriction was
7 observed in STZ-treated animals (Fig. 5A; 2-way ANOVA, $p < 0.05$). To explore whether
8 this dysfunction was also evident in microglial-mediated vessel constriction, *ex vivo* retinal
9 explants from control and STZ-treated animals (4 weeks post-STZ) were exposed to
10 fractalkine and capillary diameter quantified. While constriction was evident in the control
11 cohort, this response was absent in the STZ-treated animals (Fig. 5B, 2-way ANOVA, control
12 $p < 0.05$, STZ-treated $p = 0.99$). When microglia were isolated from 4-week STZ-treated and
13 control retinæ and RNAseq performed, angiotensinogen (*Agt*) expression was increased 2.4
14 fold, while expression of the aryl hydrocarbon receptor gene (*Ahr*), a negative regulator of the
15 RAS (42) was also increased (3.6 fold, Fig. 5C).

16
17 Based on the loss of vasomotor control in the diabetic retina and the dysregulation of the
18 microglial RAS pathway, animals were rendered diabetic and treated with candesartan
19 cilexetil or vehicle in their drinking water. At 4 weeks post-STZ, capillary diameter and
20 retinal blood flow were quantified. OCTA analysis of superficial retinal capillaries showed a
21 decrease in diameter within the vehicle control group, similar to that observed in Fig. 3I (Fig.
22 5D, $91.8 \pm 2\%$, 2-way ANOVA, $p < 0.05$). This capillary constriction was not evident in
23 STZ-treated animals exposed to candesartan, with diameters returning to control levels (Fig.
24 5D, $99.9 \pm 1.8\%$, 2-way ANOVA, $p > 0.99$). However, despite this, retinal blood flow
25 remained slower, with arterio-venous transit time increased in the vehicle and candesartan

1 STZ-treated animals (Fig. 5E; median regression analysis $p < 0.05$, $p < 0.001$ respectively).
2 Quantification of larger retinal vessels (arterioles and venules) showed systemic delivery of
3 candesartan resulted in an increase arteriovenous ratio in the STZ-treated animals compared
4 to candesartan-treated control (Fig. 5F; STZ 0.94 ± 0.01 , control 0.84 ± 0.01 , 2-way ANOVA
5 $p < 0.05$) and vehicle-treated control and STZ animals (Fig. 5F; control 0.798 ± 0.03 , STZ
6 0.86 ± 0.02 , 2-way ANOVA $p < 0.001$ and 0.05 , respectively).
7 Overall, these data show that in early diabetes, retinal vasomodulation is aberrant, with no
8 evidence of microglial mediated vasoconstriction and specific dysregulation of the RAS.
9 However, treatment with the AT1R inhibitor, candesartan, did not restore retinal blood flow,
10 despite dilating the retinal capillaries.

11

12 **Discussion**

13 The current study examined the role of microglia in local control of inner retinal blood
14 supply. Microglia preferentially contact retinal capillaries that reside in the superficial
15 vascular plexus, as well as contacting neuronal synapses within the inner retina. A novel role
16 for microglia in vasomodulation within the retina and brain was identified, where addition of
17 fractalkine induced capillary constriction. Subsequent characterisation within the retina
18 showed this vasomodulation to be dependent on microglial contact and Cx3cr1 signalling.
19 The microglial transcriptome contained gene transcripts for known vasoactive agents, while
20 the AT1R inhibitor, candesartan, blocked capillary constriction, suggesting microglial
21 vasoregulation likely occurs via modulation of local RAS. This was supported data showing
22 fractalkine-Cx3cr1-mediated upregulation of angiotensinogen. The microglial vasoregulatory
23 role was further explored in the context of vascular dysfunction during early diabetes. After 4
24 weeks of experimental diabetes, retinal blood flow was reduced, coincident with constriction
25 of the retinal capillaries within the superficial plexus and increased microglial-capillary

1 association. However, there was no indication of classical microglial activation, nor a more
2 generalised macroglial response during this early stage of diabetes. RNAseq data showed
3 altered microglial expression of components of the RAS and there was a loss of microglial-
4 mediated capillary constriction during diabetes. Finally, treatment with candesartan restored
5 retinal capillary diameter in STZ-treated animals, however, retinal blood flow remained
6 reduced.

7

8 **Microglial vasomodulation within the retina.**

9 The current data show that microglia are intimately associated with retinal vasculature,
10 directly opposing pericytes and capillary areas free from pericytes, yet showing no particular
11 preference for direct contact. Highlighting the functional significance of this interaction,
12 stimulation of the microglial specific receptor Cx3cr1 via its sole ligand fractalkine, induced
13 vasoconstriction, not only within the mouse and rat retina, but also in the brain. While the
14 role of fractalkine-induced vessel constriction in the brain requires significantly more work to
15 confirm microglial / Cx3cr1 involvement in areas exhibiting constriction, within the retina
16 this effect was spatially discrete, occurring only in areas associated with microglial processes
17 and was dependent on Cx3cr1 signalling, with *Cx3cr1^{GFP/GFP}* retinae exhibiting no
18 constriction, altered microglia-vessel contact and capillary diameter. These data directly
19 implicate microglia in the capillary response to fractalkine. While previous work has
20 identified microglia as a component of the blood-brain barrier (43), and involved in retinal
21 and brain vascular development (44, 45), this is the first report of microglial-mediated
22 vasomodulation. Furthermore, our data and those of others show microglia also monitor and
23 modulate neuronal synapses during development, throughout adulthood and in response to
24 activity (17, 46, 47), raising the possibility that microglia may contribute to neurovascular
25 coupling, the process through which local blood flow is regulated by neuronal activity. As

1 previous work in the retina suggests the existence of Müller cell-independent vasoregulatory
2 mechanisms (11, 12), microglial vasoregulation may constitute one such alternative pathway,
3 particularly within the superficial plexus. Further work exploring the structure of microglial-
4 neuronal contact, it's temporal characteristics and its response to altered neuronal activity
5 will be required to properly characterise the role of microglia in the neurovascular unit.

6

7 **Microglial RAS involvement in capillary constriction**

8 In order for microglia to directly mediate vessel constriction, they must express vasoactive
9 factors. The RNAseq data from isolated retinal microglia highlighted several genes for
10 vasoactive agents, including endothelin (*Edn1*, 3), angiotensinogen (*Agt*) and arachidonate 5-
11 lipoygenase (*Alox5*), all of which are known to regulate retinal capillary tone (48). While
12 retinal neuronal / glial cell contamination may confound the genes identified within the
13 microglial isolate, the low levels of neuronal signature genes (Fig. S5) suggest any effect
14 would be minor. Importantly, pre-incubation with the AT1R antagonist, candesartan,
15 inhibited microglial-mediated vasoconstriction and incubation with fractalkine induced up
16 regulation of microglial *Agt* expression which was not observed when *Cx3cr1* was genetically
17 ablated (*Cx3cr1*^{GFP/GFP}). These data together with the dysregulated microglial genes
18 identified during diabetes (*Agt* and *Ahr*), implicate the RAS in microglial-mediated
19 vasoregulation. All components of the RAS have been observed within the retina, with
20 angiotensin II (AngII) implicated in the vasoconstriction of all retinal vessels (arterioles,
21 capillaries and venules) via AT1R (30, 31). While this microglial-mediated vasoregulation
22 via the RAS is novel, microglia are known to express components of this pathway, including
23 angiotensin converting enzyme, AT1R, AT2R (49). In addition to vessel constriction via the
24 microglial RAS, microglial activation and inflammatory cytokine production has been
25 described after AngII exposure within the brain and retina (50, 51). Thus, the modulation of

1 the microglial RAS in normal tissue may be required for normal vessel control, whilst during
2 pathology there may be a positive feedback cycle involving AngII, promoting microglial
3 activation and inflammation.

4

5 Given the ultrastructural and immunocytochemical data suggesting microglia contact pericyte
6 somata and processes, it is possible that microglia communicate directly with pericytes and
7 utilise their vasomodulatory capacity (5) in order to constrict inner retinal capillaries.
8 Supporting communication between both cell types, pericytes are able to modulate microglial
9 phenotype during inflammation (52), while AT1R are expressed by pericytes enabling AngII-
10 mediated constriction (31). In addition to pericytes, our data also show that microglia could
11 elicit a response by communicating directly with endothelial cells (capillary areas free of
12 pericytes), which are also known to express vasoregulatory substances (53). Finally,
13 microglia may indirectly communicate with vessels via other retinal glia such as Müller cells,
14 which express components of the RAS (54) and have been previously shown to regulate the
15 inner retinal vasculature (9, 10). While a proposed mechanism is shown in Fig. 6, more work
16 is required to explain how microglia signal to other members of the neurovascular unit to
17 induce capillary constriction.

18

19 **Microglial involvement in capillary constriction during early diabetes and its effect on** 20 **retinal blood flow**

21 Our finding of reduced retinal blood flow throughout all retinal vessel types in response to
22 short duration hyperglycaemia is supported by studies in both humans with diabetes and
23 animal models of the disease (24). In contrast to larger retinal vessels which showed no
24 alteration, a significant reduction in capillary diameter (~ -9%) within the superficial plexus
25 was observed. To our knowledge this is a novel finding and while the change in capillary

1 diameter is small, it would lead to large effect on blood flow, since capillaries constitute the
2 majority of retinal vasculature (55). One estimate indicated a 6% dilation in capillary
3 diameter (~0.32 μm) generated the majority of blood flow increase evoked by neuronal
4 activity (5). In addition to static vessel change, retinal capillaries from STZ-treated animals
5 failed to constrict after hyperoxic challenge. This is the first report of *in vivo* retinal capillary
6 diameter measurement during vascular challenge, however, previous human studies have
7 reported altered hyperoxic retinal vessel responses (blood flow) in patients with type 1 (56)
8 and type 2 (57) diabetes.

9
10 As changes in the capillary network have been suggested to underlie the pathophysiology of
11 early and later stage DR (24, 58, 59), it is tempting to speculate that microglial control of
12 these vessels contribute to the vascular dysfunction in early diabetes. The data showing an
13 increase in the number of microglial processes associated with the capillary network, the
14 increase in microglial angiotensinogen (*Agt*) expression and the restoration of capillary
15 diameter after candesartan cilexetil treatment all support this hypothesis. Even the increased
16 microglial expression of aryl hydrocarbon receptor (*Ahr*), a negative regulator of
17 vasoconstriction (42), may be incorporated into this theory, since recent work shows it
18 contributes to vessel stiffness (60). Therefore, the increased *Ahr* and *Agt* expression may
19 contribute to the phenotype of smaller and less responsive retinal blood vessels in early
20 diabetes. Additional support for a microglial-specific effect on the retinal vasculature during
21 diabetes comes from work undertaken in STZ-treated *Cx3cr1^{GFP/GFP}* animals, which showed
22 increased acellular capillaries after 4 months of hyperglycaemia (61). Further work using the
23 STZ-treated *Cx3cr1^{GFP/GFP}* model is required to specifically explore the capillary constriction
24 evidenced early in diabetes.

25

1 The microglial dysregulation of the RAS suggests this pathway is altered in diabetes. These
2 data are supported by our supplementary data (*SI appendix*, Fig. S9) and previous studies
3 showing increased angiotensinogen within the vitreous of individuals with proliferative DR
4 (62) and increased vitreal AngII concentrations and elevated retinal AngII, AT1R and AT2R
5 levels in rodent models of diabetes (63, 64). As well as causing vasoconstriction, AngII is
6 also known to uncouple pericytes from the endothelium, thereby altering vessel permeability
7 and contributing to the development of microaneurysms, a key clinical determinant of DR
8 (31). Validating the positive effects of candesartan on capillary vessel diameter and providing
9 further support for the role of the RAS in DR, an earlier clinical trial showed candesartan
10 blockade to be successful in preventing the onset of clinical grade DR in individuals with
11 diabetes without DR (65). As these beneficial effects did not extend to preventing progression
12 of DR in those with the disease, it suggests dysregulation of the RAS is relevant to the early,
13 preclinical stage of DR.

14

15 Therefore, when the current data is considered together with the literature showing the RAS
16 dysregulation during diabetes and the several studies showing increased fractalkine protein
17 levels in the retina of STZ-treated rats (66, 67), a hypothesis can be formulated whereby in
18 early diabetes, increased fractalkine expression together with enhanced microglial process-
19 capillary interaction and a dysregulated microglial RAS, result in increased capillary
20 vasoconstriction. While this potential role of microglial vasoregulation in DR is novel and
21 unlike its inflammatory roles later in disease (39), further work is required to fully understand
22 this early dysfunction and how it contributes to later pathology such as the diminished
23 hyperaemic response observed in patients with diabetes (68, 69) and retinal hypoxia leading
24 to later stage DR (36, 70).

25

1 While candesartan blockade did restore retinal capillary diameter to control levels in the
2 current study, retinal blood flow remained decreased. This was surprising, as reversing
3 capillary constriction would be expected to increase retinal blood flow, given the importance
4 of the microvasculature (5, 55) and previous work showed candesartan cilexetil to restore
5 blood flow in diabetic rats, all be it after 2 weeks post-STZ (71). However, quantification of
6 arteriovenous ratio in the candesartan-treated STZ animals showed increased diameter of
7 these larger vessels. These data, in conjunction with previous work which showed
8 angiotensin II-dependent constriction of arterioles and venules (72), suggest that the dilation
9 of the larger retinal vessels in the candesartan-treated STZ animals may result in reduced
10 retinal blood velocity which masked the effect of the dilated capillaries. A more targeted
11 delivery of factors for microglial RAS blockade may overcome these confounds and provide
12 a clearer picture with respect to capillary dilation and retinal blood flow.

13

14 In summary, this study identifies a novel role for microglia in the modulation of capillaries
15 within the CNS, particularly the retina. It highlights the involvement of the fractalkine-
16 Cx3cr1 signalling axis and implicates the RAS in microglial-mediated capillary
17 vasoregulation in the normal tissue and during the early stages of DR. While inhibition of the
18 RAS pathway alters capillary constriction, it does not alter overall retinal blood flow in early
19 diabetes. Further work investigating the cellular mechanism of microglial-induced
20 vasoconstriction and intercellular signalling between microglia and other components of the
21 neurovascular unit, will provide valuable information on the retinal vascular response in
22 health and disease.

23

24 **Materials and Methods**

25 **Animals**

1 Animal procedures were approved by the University of Melbourne Ethics Committee
2 (#1613867) and adhered to the National Health and Medical Research Council of Australia
3 guidelines and the Guide for the Care and Use of Laboratory Animals. To explore the role of
4 microglia in retinal vasomodulation, *Cx3cr1^{GFP/+}* and *Cx3cr1^{GFP/GFP}* mice were used which
5 have one or both alleles of the monocyte-specific receptor, *Cx3cr1*, replaced with enhanced
6 green fluorescent protein (EGFP) (73). To show that *Cx3cr1* labels microglia within healthy
7 retina and not infiltrating monocytes, immunohistochemistry was performed with select
8 markers (*SI appendix*, Fig. S1). NG2-DsRed pericyte reporter mice were used to explore
9 pericyte-microglial contact and were provided by Dr Sagdullaev. Adult mice were
10 anaesthetised (ketamine:xylazine 67:13 mg/kg) and processed for transmission electron
11 microscopy, live cell imaging or immunohistochemistry. Hyperglycaemia was induced in
12 male adult (6 – 8-week-old) dark agouti rats via a single intraperitoneal injection of
13 streptozotocin (STZ, 55 mg/kg, in trisodium citrate buffer, pH 4.5, Sigma-Aldrich Co, MO,
14 USA), with control animals receiving an equivalent volume of vehicle. Blood glucose was
15 measured 24 hours after injection to confirm conversion (>12 mmol/L; Accu-Chek Go,
16 Roche Diagnostics, North Ryde, Australia). Weight and blood glucose levels were measured
17 biweekly and STZ-treated animals received 2 units of insulin subcutaneously when blood
18 glucose was ≥ 30 mmol/L (Novartis Pharmaceuticals Australia Pty. Ltd., North Ryde,
19 Australia). A separate cohort of animals was treated with candesartan cilexetil (10 μ g/ml;
20 Sigma-Aldrich, #SML0245) or vehicle (PEG400 / Ethanol / Kolliphor® EL / water,
21 10:5:2:83, Sigma-Aldrich) in their drinking water, 24 hours after diabetes induction. After
22 four weeks of diabetes, general anaesthesia was induced with an intraperitoneal injection of
23 ketamine and xylazine (60 and 5 mg/kg respectively, Troy Laboratories Pty Ltd, Smithfield,
24 Australia) prior to surgery, *in vivo* imaging and tissue isolation.

25

1 **Live cell imaging**

2 Anesthetised *Cx3cr1*^{GFP/+} and *Cx3cr1*^{GFP/GFP} animals (n = 5, 6 respectively) were injected
3 intraperitoneally with rhodamine B (Sigma-Aldrich) to label blood vessels, since IB4
4 labelling on live cell explants showed microglia cross reactivity (*SI appendix*, Fig. S4). After
5 5 minutes, animals were overdosed (pentobarbitone phosphate, 120 mg/kg) and retinae
6 dissected into chilled Ames medium (Sigma-Aldrich) pre-bubbled with carbogen gas (95%
7 O₂, 5% CO₂). Retinae were imaged on an inverted confocal microscope (Leica SP5), perfused
8 with 37°C carbogenated Ames at 1ml/minute. Recombinant rat fractalkine (200 ng/ml; R&D
9 Systems, MN, USA, #537-FT-025/CF) or vehicle (PBS) was introduced after 10 minutes of
10 baseline recording and imaged for a further 10 minutes. At the end of this incubation, vessel
11 diameter was measured at sites with or without microglial contact and measurements
12 expressed as a percentage of baseline diameter of the same vessel region (taken as the
13 average vessel diameter over the initial 10 minute baseline). *Ex vivo* preparations were
14 imaged for a total of 30 minutes to limit vessel calibre variability. While this *ex vivo*
15 preparation may have limitations with respect to retinal blood flow, all explants were treated
16 identically and all effects were relative to initial baseline. The vascular response to fractalkine
17 after 4 weeks of STZ-induced diabetes was measured using the above protocol, while to
18 assess the role of the RAS in fractalkine induced constriction, *ex vivo* retinae were pre-
19 incubated in Ames or Ames + 230 nM candesartan cilexetil (Sigma-Aldrich) for 10 minutes.
20 Fractalkine (200ng/ml) was subsequently added and imaged for 10 minutes (n = 5 fractalkine
21 + candesartan; n=7 fractalkine), at which time vessel diameter was quantified relative to pre-
22 incubation baseline. While candesartan cilexetil is a prodrug that is generally activated during
23 gastrointestinal absorption, carboxyl esterases are present within the retina (74) and our
24 previous work shows candesartan cilexetil blocks angiotensin-induced vessel effects when
25 delivered directly to the eye (51).

1

2 ***In vivo* video fluorescein angiography**

3 For blood flow kinetic analysis of diabetic animals, *in vivo* video fluorescein angiography
4 (VFA) was performed (n = 21 / group) as described previously using the Micron III rodent
5 imaging system (Phoenix Research Labs, CA, USA) (33). This technique provides reliable
6 quantification of blood flow kinetics using sodium fluorescein (1%, 100 µl/kg, Fluorescite
7 10%, Alcon Laboratories, NSW, Australia). Additional details are provided in the *SI*
8 *appendix*. The time taken from fluorescein entry into the retina to half-maximum intensity
9 (fill time), and the time taken to fall from maximum intensity to the midpoint between
10 maximum and final intensity after 30 seconds of imaging (drain time) were recorded.

11

12 ***In vivo* Optical Coherence Tomography Angiography**

13 To assess capillary diameter and capillary hyperoxic response *in vivo*, Optical Coherence
14 Tomography Angiography (OCTA) was performed (OCT2 Spectralis, Heidelberg
15 Engineering, Heidelberg, Germany). OCTA uses motion contrast imaging to generate real-
16 time angiographic maps of the retinal vasculature (75). Volume scans (15 x 15-degree region
17 of interest) were taken 2 – 3 disc diameters from the optic nerve. Each region consisted of
18 512 B-scans with each B-scan consisting of 512 A-scans. Superior and inferior retina were
19 scanned in both eyes. The vascular response to hyperoxic conditions was measured in 4-week
20 STZ-treated and control animals by exposing the animal to 100% oxygen via a nose cone (3
21 L/min). After a baseline image was taken, follow-up mode was used to acquire a second
22 capillary image in the same retinal location, after 2 minutes of oxygen breathing.

23

24 **Immunocytochemistry**

1 Rat or mouse retinae were processed for indirect immunofluorescence in wholemount or
2 cross section, as previously described (76). Human tissue was obtained and processed as
3 described previously (77). Retinal microglia were labelled with rabbit anti-ionized calcium-
4 binding adapter molecule 1 (Iba-1,1:1000; Wako, Osaka, Japan) or expressed EGFP
5 (*Cx3cr1^{GFP/+}*, *Cx3cr1^{GFP/GFP}*), while blood vessels were visualised with *Griffonia*
6 *simplicifolia* isolectin B4 (IB4, FITC 1:75; Sigma-Aldrich; 647 fluorophore 1:100; Thermo
7 Fisher Scientific, MA, USA). While IB4 has shown cross reactivity with brain microglia and
8 activated retinal microglia (78, 79), we observe no cross reactivity in any fixed retinal tissues.
9 We also show better vessel coverage using IB4 compared to the endothelial marker CD-31
10 (*SI appendix*, Fig. S10). Further details for immunolabelling are in *SI appendix*. All imaging
11 was performed with a 20X objective on either Zeiss META / LSM800 confocals (Carl Zeiss,
12 Oberkochen, Germany) or Leica SP5 (Wetzlar, Germany), while high resolution imaging of
13 microglial-pericyte contact and EGFP expressing microglia was performed at 63X. For
14 subsequent analysis of retinal wholemounts, tile scans were taken at the superficial vascular
15 plexus with z-stacks (15.6µm) used to accommodate the variations in retinal mounting. All
16 subsequent image analysis was performed on maximum intensity projections.

17

18 **Image analysis**

19 **Vessel morphology:** Fundus images (n = 13 / group) were analysed for arteriole / venule
20 width and tortuosity in MATLAB (Mathworks Inc., MA, USA) using the open source plugin
21 ARIA (80) at an eccentricity of 1.5 and 2 disc diameters from the optic nerve. Capillary width
22 (<15 µm) within the superficial vascular plexus (OCTA) was measured using AngioTool
23 (81). Confocal wholemount images (n = 11 animals / group) were grouped into arterioles,
24 venules and capillaries based on their corresponding VFA profile and vessel masks used to
25 segment subsequent analysis in Metamorph (Molecular devices, CA, USA) using the

1 angiogenesis tube formation application. Total vessel area was quantified in NIH ImageJ (82)
2 for each vessel type and vessel density was expressed as percentage of vessel area covering
3 the total retinal area. For all subjective measurements, individuals were blinded to the
4 treatment group.

5

6 **Microglial, glial, pericyte histology and vessel interaction:** Microglia, pericytes and
7 astrocytes from STZ-treated and control tissue were analysed in Metamorph utilising the
8 neurite outgrowth application. Iba-1 positive microglia were segmented, counted and a mask
9 generated. This microglial mask was overlaid on the vessel / pericyte masks and cells that
10 overlapped with blood vessels by at least $0.82\mu\text{m}$ were considered touching and were
11 calculated as a percentage of total cells. For microglial blood vessel and neuronal contact in
12 *Cx3cr1^{GFP/+}* and *Cx3cr1^{GFP/GFP}* retinae, areas of colocalization between individual microglia
13 and vessels and synapses were rendered as a 3D volume and expressed as a percentage of the
14 total volume of the microglial cell (Imaris, Bitplane, Zurich, Switzerland; 3 microglia /
15 quadrant / retina, n = 5 animals / genotype). To further characterise microglial-pericyte
16 interaction a custom Metamorph script was used to quantify contacts (within $0.41\mu\text{m}$)
17 between microglia (Iba-1 positive) with pericyte somata and processes (NG2 positive), as
18 well as capillary areas devoid of pericyte contact (NG2 negative, IB4 positive). Previous
19 work has used EGFP in order to assess microglial contact with neurons in the retina and brain
20 (17, 46, 83). Microglial morphology was also quantified using the automated neurite
21 outgrowth application (Metamorph), while microglial-neuronal synapse and microglial-
22 pericyte images were processed in Imaris. Astrocyte density within the ganglion cell layer
23 was quantified for total retinal area and for overlap with each vessel type. Müller cell gliosis
24 was quantified as previously described (84) (3 sections / animal, n = 6 animals).

25

1 **Electron microscopy**

2 Pre-embedding immuno-electron microscopy was used to investigate the ultrastructural
3 association of inner retinal capillaries and microglia in the *Cx3cr1*^{GFP/+} retina, as previously
4 described (76). The immunolabelling of EGFP using this protocol shows that EGFP is present
5 close (<50nm) to the membrane at the tips of microglial processes (Fig. 1C).

7 **Microglial isolation and RNA-Seq**

8 Retinae from control and 4-week STZ-treated rats (n = 5 control, n = 4 STZ, 12 weeks-old)
9 were isolated, papain digested (Worthington Biochemical, NJ, USA), and labelled with
10 CD11b-FITC conjugate (Miltenyi Biotec, Bergisch Gladbach, Germany) for microglial
11 isolation (FACSaria III, BD Bioscience, San Jose, USA). RNA was isolated and RNAseq
12 performed as in *SI appendix*. The identified microglial gene population was compared to
13 other studies reporting microglial-enriched genes, as well as those detailing neuronal
14 signature genes (*SI appendix*, Fig. S5). The RNAseq dataset was deposited into Gene
15 Expression Omnibus (#GSE 139276). To explore fractalkine regulation of microglial RAS,
16 retinae from C57bl6 and *Cx3cr1*^{GFP/GFP} animals (n = 6) were incubated as above with
17 fractalkine (200ng/ml, R&D Systems) or PBS for 2 hours at 37°C. Retinal microglia were
18 isolated via FACS using the CD11b and EGFP labels. RNA was isolated and Smart-seq 2
19 performed with 13 cycles of pre-amplification followed by quantitative PCR (see *SI*
20 *appendix*).

22 **Statistical analysis**

23 Statistical significance was determined by two-tailed unpaired student's t-test, two-way
24 ANOVA or RM-ANOVA depending on the experiment (Prism 6.0, GraphPad, CA, USA).
25 Where required a Tukey post-hoc analysis was performed. Blood flow analysis was

1 undertaken using median regression analysis (STATA, StataCorp TX, USA). Alpha levels
2 were set at 0.05. Numerical values are expressed as mean \pm standard error of mean (SEM)
3 unless otherwise stated.

4

1 **Acknowledgements**

2 The authors thank Dr Leonid Churilov for his assistance with statistical analysis, Dr Christine
3 Nguyen and Mr Darren Zhao for their assistance with blood gas analysis and Ms Satya
4 Gunnam for her assistance with immunohistochemical staining and analysis. We also
5 acknowledge the Biological Optical Microscopy and Cytometry Platforms at the University
6 of Melbourne.

7

References

1. Ames A, 3rd, Li YY, Heher EC, Kimble CR. Energy metabolism of rabbit retina as related to function: high cost of Na⁺ transport. *J Neurosci.* 1992;12(3):840-53.
2. Yu DY, Cringle SJ. Oxygen distribution and consumption within the retina in vascularised and avascular retinas and in animal models of retinal disease. *Prog Retin Eye Res.* 2001;20(2):175-208.
3. Campbell JP, Zhang M, Hwang TS, Bailey ST, Wilson DJ, Jia Y, et al. Detailed Vascular Anatomy of the Human Retina by Projection-Resolved Optical Coherence Tomography Angiography. *Sci Rep.* 2017;7:42201.
4. Kornfield TE, Newman EA. Regulation of blood flow in the retinal trilaminar vascular network. *J Neurosci.* 2014;34(34):11504-13.
5. Hall CN, Reynell C, Gesslein B, Hamilton NB, Mishra A, Sutherland BA, et al. Capillary pericytes regulate cerebral blood flow in health and disease. *Nature.* 2014;508(7494):55-60.
6. Riva CE, Logean E, Falsini B. Visually evoked hemodynamical response and assessment of neurovascular coupling in the optic nerve and retina. *Prog Retin Eye Res.* 2005;24(2):183-215.
7. Metea MR, Newman EA. Signalling within the neurovascular unit in the mammalian retina. *Exp Physiol.* 2007;92(4):635-40.
8. Takano T, Tian GF, Peng W, Lou N, Libionka W, Han X, et al. Astrocyte-mediated control of cerebral blood flow. *Nat Neurosci.* 2006;9(2):260-7.
9. Newman EA. Calcium increases in retinal glial cells evoked by light-induced neuronal activity. *J Neurosci.* 2005;25(23):5502-10.
10. Newman EA. Functional hyperemia and mechanisms of neurovascular coupling in the retinal vasculature. *J Cereb Blood Flow Metab.* 2013;33(11):1685-95.
11. Biesecker KR, Srienc AI, Shimoda AM, Agarwal A, Bergles DE, Kofuji P, et al. Glial Cell Calcium Signaling Mediates Capillary Regulation of Blood Flow in the Retina. *J Neurosci.* 2016;36(36):9435-45.
12. Mishra A, Hamid A, Newman EA. Oxygen modulation of neurovascular coupling in the retina. *Proc Natl Acad Sci U S A.* 2011;108(43):17827-31.
13. Filosa JA, Morrison HW, Iddings JA, Du W, Kim KJ. Beyond neurovascular coupling, role of astrocytes in the regulation of vascular tone. *Neuroscience.* 2016;323:96-109.
14. Grigsby JG, Cardona SM, Pouw CE, Muniz A, Mendiola AS, Tsin AT, et al. The role of microglia in diabetic retinopathy. *J Ophthalmol.* 2014;2014:705783.
15. Tang J, Kern TS. Inflammation in diabetic retinopathy. *Prog Retin Eye Res.* 2011;30(5):343-58.
16. Hanisch UK, Kettenmann H. Microglia: active sensor and versatile effector cells in the normal and pathologic brain. *Nat Neurosci.* 2007;10(11):1387-94.
17. Tremblay ME, Lowery RL, Majewska AK. Microglial interactions with synapses are modulated by visual experience. *PLoS Biol.* 2010;8(11):e1000527.
18. Tremblay ME, Majewska AK. A role for microglia in synaptic plasticity? *Commun Integr Biol.* 2011;4(2):220-2.
19. Lee JE, Liang KJ, Fariss RN, Wong WT. Ex vivo dynamic imaging of retinal microglia using time-lapse confocal microscopy. *Invest Ophthalmol Vis Sci.* 2008;49(9):4169-76.
20. Tan B, Mason E, MacLellan B, Bizheva KK. Correlation of Visually Evoked Functional and Blood Flow Changes in the Rat Retina Measured With a Combined OCT+ERG System. *Invest Ophthalmol Vis Sci.* 2017;58(3):1673-81.
21. Cheung N, Mitchell P, Wong TY. Diabetic retinopathy. *The Lancet.* 2010;376(9735):124-36.
22. Tayyari F, Khuu LA, Flanagan JG, Singer S, Brent MH, Hudson C. Retinal Blood Flow and Retinal Blood Oxygen Saturation in Mild to Moderate Diabetic Retinopathy. *Invest Ophthalmol Vis Sci.* 2015;56(11):6796-800.
23. Bursell SE, Clermont AC, Kinsley BT, Simonson DC, Aiello LM, Wolpert HA. Retinal blood flow changes in patients with insulin-dependent diabetes mellitus and no diabetic retinopathy. *Invest Ophthalmol Vis Sci.* 1996;37(5):886-97.
24. Clermont AC, Bursell SE. Retinal blood flow in diabetes. *Microcirculation.* 2007;14(1):49-61.

- 1 25. Cheung CY, Ikram MK, Klein R, Wong TY. The clinical implications of recent studies on the
2 structure and function of the retinal microvasculature in diabetes. *Diabetologia*. 2015;58(5):871-85.
- 3 26. Dudvarski Stankovic N, Teodorczyk M, Ploen R, Zipp F, Schmidt MHH. Microglia-blood vessel
4 interactions: a double-edged sword in brain pathologies. *Acta Neuropathol*. 2016;131(3):347-63.
- 5 27. Zieger M, Ahnelt PK, Uhrin P. CX3CL1 (fractalkine) protein expression in normal and
6 degenerating mouse retina: in vivo studies. *PLoS One*. 2014;9(9):e106562.
- 7 28. Gyoneva S, Hosur R, Gosselin D, Zhang B, Ouyang Z, Coteleur AC, et al. Cx3cr1-deficient
8 microglia exhibit a premature aging transcriptome. *Life Sci Alliance*. 2019;2(6).
- 9 29. Chiu IM, Morimoto ET, Goodarzi H, Liao JT, O'Keeffe S, Phatnani HP, et al. A
10 neurodegeneration-specific gene-expression signature of acutely isolated microglia from an
11 amyotrophic lateral sclerosis mouse model. *Cell Rep*. 2013;4(2):385-401.
- 12 30. Rockwood EJ, Fantès F, Davis EB, Anderson DR. The response of retinal vasculature to
13 angiotensin. *Invest Ophthalmol Vis Sci*. 1987;28(4):676-82.
- 14 31. Kawamura H, Kobayashi M, Li Q, Yamanishi S, Katsumura K, Minami M, et al. Effects of
15 angiotensin II on the pericyte-containing microvasculature of the rat retina. *J Physiol*. 2004;561(Pt
16 3):671-83.
- 17 32. Mishra A, Newman EA. Inhibition of inducible nitric oxide synthase reverses the loss of
18 functional hyperemia in diabetic retinopathy. *Glia*. 2010;58(16):1996-2004.
- 19 33. Hui F, Nguyen CT, Bedgood PA, He Z, Fish RL, Gurrell R, et al. Quantitative spatial and
20 temporal analysis of fluorescein angiography dynamics in the eye. *PLoS One*. 2014;9(11):e111330.
- 21 34. Yau JW, Rogers SL, Kawasaki R, Lamoureux EL, Kowalski JW, Bek T, et al. Global prevalence
22 and major risk factors of diabetic retinopathy. *Diabetes Care*. 2012;35(3):556-64.
- 23 35. Broe R, Rasmussen ML, Frydkjaer-Olsen U, Olsen BS, Mortensen HB, Hodgson L, et al. Retinal
24 vessel calibers predict long-term microvascular complications in type 1 diabetes: the Danish Cohort
25 of Pediatric Diabetes 1987 (DCPD1987). *Diabetes*. 2014;63(11):3906-14.
- 26 36. Ly A, Yee P, Vessey KA, Phipps JA, Jobling AI, Fletcher EL. Early inner retinal astrocyte
27 dysfunction during diabetes and development of hypoxia, retinal stress, and neuronal functional
28 loss. *Invest Ophthalmol Vis Sci*. 2011;52(13):9316-26.
- 29 37. Rungger-Brandle E, Dosso AA, Leuenberger PM. Glial reactivity, an early feature of diabetic
30 retinopathy. *Invest Ophthalmol Vis Sci*. 2000;41(7):1971-80.
- 31 38. Carmo A, Cunha-Vaz JG, Carvalho AP, Lopes MC. Effect of cyclosporin-A on the blood--retinal
32 barrier permeability in streptozotocin-induced diabetes. *Mediators Inflamm*. 2000;9(5):243-8.
- 33 39. Zeng XX, Ng YK, Ling EA. Neuronal and microglial response in the retina of streptozotocin-
34 induced diabetic rats. *Vis Neurosci*. 2000;17(3):463-71.
- 35 40. Holtman IR, Raj DD, Miller JA, Schaafsma W, Yin Z, Brouwer N, et al. Induction of a common
36 microglia gene expression signature by aging and neurodegenerative conditions: a co-expression
37 meta-analysis. *Acta Neuropathol Commun*. 2015;3:31.
- 38 41. Feng C, Wang X, Liu T, Zhang M, Xu G, Ni Y. Expression of CCL2 and its receptor in activation
39 and migration of microglia and monocytes induced by photoreceptor apoptosis. *Mol Vis*.
40 2017;23:765-77.
- 41 42. Lund AK, Goens MB, Kanagy NL, Walker MK. Cardiac hypertrophy in aryl hydrocarbon
42 receptor null mice is correlated with elevated angiotensin II, endothelin-1, and mean arterial blood
43 pressure. *Toxicol Appl Pharmacol*. 2003;193(2):177-87.
- 44 43. Zlokovic BV. The blood-brain barrier in health and chronic neurodegenerative disorders.
45 *Neuron*. 2008;57(2):178-201.
- 46 44. Checchin D, Sennlaub F, Levavasseur E, Leduc M, Chemtob S. Potential role of microglia in
47 retinal blood vessel formation. *Invest Ophthalmol Vis Sci*. 2006;47(8):3595-602.
- 48 45. Arnold T, Betsholtz C. Correction: The importance of microglia in the development of the
49 vasculature in the central nervous system. *Vasc Cell*. 2013;5(1):12.

- 1 46. Schafer DP, Lehrman EK, Kautzman AG, Koyama R, Mardinly AR, Yamasaki R, et al. Microglia
2 sculpt postnatal neural circuits in an activity and complement-dependent manner. *Neuron*.
3 2012;74(4):691-705.
- 4 47. Wang X, Zhao L, Zhang J, Fariss RN, Ma W, Kretschmer F, et al. Requirement for Microglia for
5 the Maintenance of Synaptic Function and Integrity in the Mature Retina. *J Neurosci*.
6 2016;36(9):2827-42.
- 7 48. Pournaras CJ, Rungger-Brandle E, Riva CE, Hardarson SH, Stefansson E. Regulation of retinal
8 blood flow in health and disease. *Prog Retin Eye Res*. 2008;27(3):284-330.
- 9 49. Liu SJ, Liu XY, Li JH, Guo J, Li F, Gui Y, et al. Gastrodin attenuates microglia activation through
10 renin-angiotensin system and Sirtuin3 pathway. *Neurochem Int*. 2018;120:49-63.
- 11 50. Torika N, Asraf K, Roasso E, Danon A, Fleisher-Berkovich S. Angiotensin Converting Enzyme
12 Inhibitors Ameliorate Brain Inflammation Associated with Microglial Activation: Possible Implications
13 for Alzheimer's Disease. *J Neuroimmune Pharmacol*. 2016;11(4):774-85.
- 14 51. Phipps JA, Vessey KA, Brandli A, Nag N, Tran MX, Jobling AI, et al. The Role of Angiotensin
15 II/AT1 Receptor Signaling in Regulating Retinal Microglial Activation. *Invest Ophthalmol Vis Sci*.
16 2018;59(1):487-98.
- 17 52. Matsumoto J, Takata F, Machida T, Takahashi H, Soejima Y, Funakoshi M, et al. Tumor
18 necrosis factor-alpha-stimulated brain pericytes possess a unique cytokine and chemokine release
19 profile and enhance microglial activation. *Neurosci Lett*. 2014;578:133-8.
- 20 53. Hamilton K, Dunning L, Ferrell WR, Lockhart JC, MacKenzie A. Endothelium-derived
21 contraction in a model of rheumatoid arthritis is mediated via angiotensin II type 1 receptors. *Vascul*
22 *Pharmacol*. 2018;100:51-7.
- 23 54. Downie LE, Vessey K, Miller A, Ward MM, Pianta MJ, Vingrys AJ, et al. Neuronal and glial cell
24 expression of angiotensin II type 1 (AT1) and type 2 (AT2) receptors in the rat retina. *Neuroscience*.
25 2009;161(1):195-213.
- 26 55. Blinder P, Tsai PS, Kaufhold JP, Knutsen PM, Suhl H, Kleinfeld D. The cortical angiome: an
27 interconnected vascular network with noncolumnar patterns of blood flow. *Nat Neurosci*.
28 2013;16(7):889-97.
- 29 56. Harris A, Arend O, Danis RP, Evans D, Wolf S, Martin BJ. Hyperoxia improves contrast
30 sensitivity in early diabetic retinopathy. *Br J Ophthalmol*. 1996;80(3):209-13.
- 31 57. Lott ME, Slocomb JE, Gao Z, Gabbay RA, Quillen D, Gardner TW, et al. Impaired coronary and
32 retinal vasomotor function to hyperoxia in Individuals with Type 2 diabetes. *Microvasc Res*.
33 2015;101:1-7.
- 34 58. Kim AY, Chu Z, Shahidzadeh A, Wang RK, Puliafito CA, Kashani AH. Quantifying Microvascular
35 Density and Morphology in Diabetic Retinopathy Using Spectral-Domain Optical Coherence
36 Tomography Angiography. *Invest Ophthalmol Vis Sci*. 2016;57(9):OCT362-70.
- 37 59. Simonett JM, Scarinci F, Picconi F, Giorno P, De Geronimo D, Di Renzo A, et al. Early
38 microvascular retinal changes in optical coherence tomography angiography in patients with type 1
39 diabetes mellitus. *Acta Ophthalmol*. 2017.
- 40 60. Eckers A, Jakob S, Heiss C, Haarmann-Stemmann T, Goy C, Brinkmann V, et al. The aryl
41 hydrocarbon receptor promotes aging phenotypes across species. *Sci Rep*. 2016;6:19618.
- 42 61. Beli E, Dominguez JM, 2nd, Hu P, Thinschmidt JS, Caballero S, Li Calzi S, et al. CX3CR1
43 deficiency accelerates the development of retinopathy in a rodent model of type 1 diabetes. *J Mol*
44 *Med (Berl)*. 2016;94(11):1255-65.
- 45 62. Gao BB, Chen X, Timothy N, Aiello LP, Feener EP. Characterization of the vitreous proteome
46 in diabetes without diabetic retinopathy and diabetes with proliferative diabetic retinopathy. *J*
47 *Proteome Res*. 2008;7(6):2516-25.
- 48 63. Byon IS, Lee DH, Jun ES, Shin MK, Park SW, Lee JE. Effect of angiotensin II type 1 receptor
49 blocker and angiotensin converting enzyme inhibitor on the intraocular growth factors and their
50 receptors in streptozotocin-induced diabetic rats. *Int J Ophthalmol*. 2017;10(6):896-901.

- 1 64. Kim JH, Kim JH, Yu YS, Cho CS, Kim KW. Blockade of angiotensin II attenuates VEGF-mediated
2 blood-retinal barrier breakdown in diabetic retinopathy. *J Cereb Blood Flow Metab.* 2009;29(3):621-
3 8.
- 4 65. Chaturvedi N, Porta M, Klein R, Orchard T, Fuller J, Parving HH, et al. Effect of candesartan
5 on prevention (DIRECT-Prevent 1) and progression (DIRECT-Protect 1) of retinopathy in type 1
6 diabetes: randomised, placebo-controlled trials. *Lancet.* 2008;372(9647):1394-402.
- 7 66. Yeh PT, Huang HW, Yang CM, Yang WS, Yang CH. Astaxanthin Inhibits Expression of Retinal
8 Oxidative Stress and Inflammatory Mediators in Streptozotocin-Induced Diabetic Rats. *PLoS One.*
9 2016;11(1):e0146438.
- 10 67. Yeh PT, Wang LC, Chang SW, Yang WS, Yang CM, Yang CH. Effect of Fenofibrate on the
11 Expression of Inflammatory Mediators in a Diabetic Rat Model. *Curr Eye Res.* 2019;44(10):1121-32.
- 12 68. Lott ME, Slocomb JE, Shivkumar V, Smith B, Quillen D, Gabbay RA, et al. Impaired retinal
13 vasodilator responses in prediabetes and type 2 diabetes. *Acta Ophthalmol.* 2013;91(6):e462-9.
- 14 69. Mandecka A, Dawczynski J, Blum M, Muller N, Kloos C, Wolf G, et al. Influence of flickering
15 light on the retinal vessels in diabetic patients. *Diabetes Care.* 2007;30(12):3048-52.
- 16 70. Arden GB, Sivaprasad S. Hypoxia and oxidative stress in the causation of diabetic
17 retinopathy. *Curr Diabetes Rev.* 2011;7(5):291-304.
- 18 71. Horio N, Clermont AC, Abiko A, Abiko T, Shoelson BD, Bursell SE, et al. Angiotensin AT(1)
19 receptor antagonism normalizes retinal blood flow and acetylcholine-induced vasodilatation in
20 normotensive diabetic rats. *Diabetologia.* 2004;47(1):113-23.
- 21 72. Kulkarni PS, Hamid H, Barati M, Butulija D. Angiotensin II-induced constrictions are masked
22 by bovine retinal vessels. *Invest Ophthalmol Vis Sci.* 1999;40(3):721-8.
- 23 73. Jung S, Aliberti J, Graemmel P, Sunshine MJ, Kreutzberg GW, Sher A, et al. Analysis of
24 fractalkine receptor CX(3)CR1 function by targeted deletion and green fluorescent protein reporter
25 gene insertion. *Mol Cell Biol.* 2000;20(11):4106-14.
- 26 74. Duvvuri S, Majumdar S, Mitra AK. Role of metabolism in ocular drug delivery. *Curr Drug*
27 *Metab.* 2004;5(6):507-15.
- 28 75. Tang FY, Ng DS, Lam A, Luk F, Wong R, Chan C, et al. Determinants of Quantitative Optical
29 Coherence Tomography Angiography Metrics in Patients with Diabetes. *Sci Rep.* 2017;7(1):2575.
- 30 76. Vessey KA, Greferath U, Jobling AI, Phipps JA, Ho T, Waugh M, et al. Ccl2/Cx3cr1 knockout
31 mice have inner retinal dysfunction but are not an accelerated model of AMD. *Invest Ophthalmol Vis*
32 *Sci.* 2012;53(12):7833-46.
- 33 77. Jobling AI, Guymer RH, Vessey KA, Greferath U, Mills SA, Brassington KH, et al. Nanosecond
34 laser therapy reverses pathologic and molecular changes in age-related macular degeneration
35 without retinal damage. *FASEB J.* 2015;29(2):696-710.
- 36 78. Ma W, Silverman SM, Zhao L, Villasmil R, Campos MM, Amaral J, et al. Absence of TGFbeta
37 signaling in retinal microglia induces retinal degeneration and exacerbates choroidal
38 neovascularization. *Elife.* 2019;8.
- 39 79. Lunemann A, Ullrich O, Diestel A, Jons T, Ninnemann O, Kovac A, et al.
40 Macrophage/microglia activation factor expression is restricted to lesion-associated microglial cells
41 after brain trauma. *Glia.* 2006;53(4):412-9.
- 42 80. Bankhead P, Scholfield CN, McGeown JG, Curtis TM. Fast retinal vessel detection and
43 measurement using wavelets and edge location refinement. *PLoS One.* 2012;7(3):e32435.
- 44 81. Zudaire E, Gambardella L, Kurcz C, Vermeren S. A computational tool for quantitative
45 analysis of vascular networks. *PLoS One.* 2011;6(11):e27385.
- 46 82. Schneider CA, Rasband WS, Eliceiri KW. NIH Image to ImageJ: 25 years of image analysis. *Nat*
47 *Methods.* 2012;9(7):671-5.
- 48 83. Fontainhas AM, Wang M, Liang KJ, Chen S, Mettu P, Damani M, et al. Microglial morphology
49 and dynamic behavior is regulated by ionotropic glutamatergic and GABAergic neurotransmission.
50 *PLoS One.* 2011;6(1):e15973.

- 1 84. Jobling AI, Vessey KA, Waugh M, Mills SA, Fletcher EL. A naturally occurring mouse model of
2 achromatopsia: characterization of the mutation in cone transducin and subsequent retinal
3 phenotype. *Invest Ophthalmol Vis Sci*. 2013;54(5):3350-9.
- 4 85. Picelli S, Faridani OR, Bjorklund AK, Winberg G, Sagasser S, Sandberg R. Full-length RNA-seq
5 from single cells using Smart-seq2. *Nat Protoc*. 2014;9(1):171-81.

6

7

1 **Figure legends**

2 **Figure 1. Retinal microglia associate with vasculature and neuronal synapses.**

3 A: Wholemouted mouse retina ($Cx3cr1^{GFP/+}$) was labelled with anti-EGFP (microglia,
4 green), and *Griffonia simplicifolia* isolectin B4 (IB4, blood vessels, red). The highlighted
5 region is magnified showing microglial association with vessels within the superficial
6 vascular plexus (*inset*). B: The association of microglial processes with vessels of different
7 diameters within the superficial plexus was quantified relative to vessel area for each vessel
8 size and show microglia preferentially associate with capillaries. C: The ultrastructure of
9 microglia-vessel contact within the $Cx3cr1^{GFP/+}$ retina shows microglial processes
10 (immunolabelled against EGFP, black dots) adjoin pericytes, which contact the endothelial
11 cells lining the capillary lumen. D: A wholemounted retina from the NG2-DsRed pericyte
12 reporter mouse (pericyte somata, processes, red) stained with Iba-1 (microglia, green) and
13 DAPI (nuclei, blue) shows a microglial process making contact with pericyte somata. The
14 boxed region is shown in XZ and YZ orthogonal projections (above and right). E: A high
15 resolution rendered image of microglial-pericyte contact taken from asterisk in panel D. F:
16 Microglial-pericyte interaction was further probed in rat retina and the extent of contact with
17 pericyte somata, processes (NG2 +ve) and capillary areas lacking pericyte contact (NG2 -ve /
18 IB4 +ve) quantified. G: A vertical section from a $Cx3cr1^{GFP/+}$ retina labelled for blood
19 vessels (IB4, magenta), microglia (EGFP, green) neuronal synapses (VGLUT1, red) and cell
20 nuclei (DAPI, blue), showing microglial processes contact retinal vessels (asterisk) and
21 neuronal synapses (arrow heads). The boxed region was imaged at higher resolution and
22 rendered to highlight microglial-synapse interaction (*inset*). H; Neuronal-microglial-vascular
23 contact is also observed in human retina (microglia, Iba-1, green; vessels, vitronectin,
24 magenta, asterisk; neuronal synapses, VGLUT1, red, arrow heads; cell nuclei, DAPI, blue). I:
25 When neuronal-microglial contact was quantified in the $Cx3cr1^{+/GFP}$ mouse at the level of the

1 inner retina (vessels, IB4, red; microglia, EGFP, green, VGLUT1, blue), the majority of
2 microglia contact both neuronal synapses and retinal vessels. Data presented as mean \pm SEM,
3 $n=5$ (*B, F*), $n=3$ (*I inset*), * $p<0.05$, *** $p<0.001$. MC, microglia; PC, pericyte; EC,
4 endothelial cell; CL, capillary lumen; ONL, outer nuclear layer; OPL, outer plexiform layer;
5 INL, inner nuclear layer; IPL, inner plexiform layer; GCL, ganglion cell layer. Scale bars
6 $500\mu\text{m}$ (*A*), $50\mu\text{m}$ (*A inset, G, H*), $20\mu\text{m}$ (*I*), $10\mu\text{m}$ (*D*), $5\mu\text{m}$ (*E*) $0.5\mu\text{m}$ (*C*).

7

8 **Figure 2. Microglia constrict retinal capillaries via fractalkine-Cx3cr1 signalling and**
9 **express genes for vasoactive agents.**

10 *A: Ex vivo Cx3cr1^{GFP/+} retinae (EGFP; microglia, green) were labelled with Rhodamine B*
11 *(blood vessels, red) and imaged under live cell microscopy. B: The addition of fractalkine*
12 *(FKN, 200ng/ml) induced vasoconstriction at sites of microglial contact (m+. $n = 4$ PBS, $n =$*
13 *6 FKN), while no significant vessel alteration occurred in areas lacking microglial processes*
14 *(m-, $n = 5$ PBS, $n=6$ FKN). When performed on *Cx3cr1^{GFP/GFP} retinae, no constriction was*
15 *evident ($n = 5$). C: The response of brain vasculature to fractalkine was tested in rat thin skull*
16 *preparations, with constriction evident 120 seconds post-injection ($n = 3$ PBS, FKN). The*
17 *insets show representative images at baseline and after fractalkine addition. D: Retinal*
18 *microglia (EGFP, green), neuronal synapses (VGLUT1, red) and blood vessels (IB4, light*
19 *blue) were imaged in *Cx3cr1^{GFP/+} and *Cx3cr1^{GFP/GFP} animals and the extent of vascular and**
20 *neuronal contact quantified relative to microglial volume (see isolated microglia, red -*
21 *neuronal contacts; blue - vascular contacts). E: Grouped data showed *Cx3cr1^{GFP/GFP} retinae**
22 *to have reduced vascular contacts compared to *Cx3cr1^{GFP/+} retinae ($n=5$), while there was no**
23 *difference in neuronal contacts. *Cx3cr1^{GFP/GFP} microglia exhibited reduced process branching**
24 *($n=5$). F: Using *in vivo* OCTA, retinal capillary diameter was increased in *Cx3cr1^{GFP/GFP}****

1 animals compared to *Cx3cr1^{GFP/+}* retinae ($n=4$ C57Bl6, $n=6$ *Cx3cr1^{GFP/+}*, *Cx3cr1^{GFP/GFP}*),
2 while there was no alteration in the diameter of arterioles or venules (A/V ratio shown in
3 table, $n=4$ C57Bl6, $n=6$ *Cx3cr1^{GFP/+}*, $n=5$ *Cx3cr1^{GFP/GFP}*). *G*: RNAseq was performed on
4 FACS-isolated rat retinal microglia, with 268 genes identified as being angiogenic
5 (GO:0001525), while 39 genes were involved in vascular constriction and 41 genes in
6 vascular dilation (regulation of blood vessel diameter, GO:0097746). *H*: Vessel diameter was
7 quantified in rat retinal explants pre-incubated in Ames (black trace) or Ames + 230 nM
8 candesartan (red trace) for 10 minutes, after which fractalkine (FKN, 200 ng/ml) was added
9 (shaded area, representative data from 1 retina, $n = 5$ vessels). *I*: When grouped data were
10 analysed 10 minutes after fractalkine addition, constriction was abolished when pre-incubated
11 with candesartan ($n = 7$ fractalkine, $n = 5$ fractalkine + candesartan). Further supporting a role
12 for the RAS, *ex vivo* incubation with fractalkine (FKN) resulted in an increase in microglial
13 *Agt* expression, while this was not evident in the microglia isolated from *Cx3cr1^{GFP/GFP}*
14 retinae (*inset*, $n=6$). Data expressed as mean \pm SEM, * $p<0.05$, ** $p<0.01$, *** $p<0.001$,
15 **** $p<0.0001$. Scale bar 50 μ m (*A*), 15 μ m (*D*).

16

17 **Figure 3. Retinal blood flow is reduced and capillaries are constricted after 4 weeks of**
18 **diabetes.**

19 VFA was used to quantify retinal blood flow in control and STZ-treated animals. *A-C*: En
20 face heat-maps depicting fill time for arterioles, capillaries and venules, with insets showing
21 representative average normalised fluorescence intensity traces for control (black line) and
22 STZ-treated (red line) animals. *D, E*: The times taken to reach half maximum intensity (*D*, fill
23 time) and half of final value from maximum (*E*, drain time) were quantified, showing fill and
24 drain times were significantly increased in all vessel types in STZ-treated animals (unfilled

1 bars, control $n = 23$; filled bars STZ, $n = 21$). *F*: Sodium fluorescein fundus images were
2 quantified for large vessel tortuosity ($n = 13$) and arteriovenous ratio (*inset*, $n = 13$), with no
3 difference observed between STZ-treated (filled bars) and control (unfilled bars) animals. *G*:
4 Immunohistochemistry was used to quantify vascular density in control and STZ-treated
5 (unfilled and filled bars) eyes, with no difference observed between the two groups ($n = 11$).
6 The rendered image shows the segmented vessel types (*inset*, capillaries in yellow, arterioles
7 in blue and venules in cyan). *H*: OCTA was performed *in vivo* to measure capillary diameter
8 in control and STZ-treated (*inset*) animals, with the vessels measured shown in green. *I*: A
9 significant decrease was observed in the capillary diameter in STZ-treated animals ($n = 12$)
10 compared to control ($n = 10$) within the superior vascular plexus. No alteration was observed
11 in the intermediate/deep vascular plexi. Group data expressed as mean \pm SEM. * $p < 0.05$.
12 Scale bars 500 μm (*A*), 1 mm (*G*), 50 μm (*H*).

13

14 **Figure 4. Microglia increase their contact with retinal capillaries after 4 weeks of STZ-**
15 **induced diabetes.**

16 *A*: Wholemouted retina from control (*inset*) and STZ-treated animals were labelled for Iba-1
17 (microglia, green) and IB4-FITC (blood vessels, red) and the extent of contact between
18 microglia and vasculature quantified for each vessel type. While no difference in large vessel
19 contacts occurred, microglia-capillary contact increased in the central retina of the STZ-
20 treated animals (filled bars, $n = 11$). *B*: Control (*inset*) and STZ-treated animals were labelled
21 for Iba-1 (microglia, green), NG2 (pericytes, light blue) and IB4-FITC (blood vessels, red)
22 and the extent of microglia-pericyte contact quantified for each vessel type. Microglial-
23 pericyte association increased within the central retina of STZ-treated animals (filled bars, n
24 = 11). *C*: Using similar immunolabelling as in *B*, microglial association with pericyte somata,

1 processes and capillary areas lacking pericyte contact was quantified. The image analysis
2 render (*inset*) highlights pericyte somata (red), pericyte processes (green) and pericyte-free
3 vessels (blue), while microglia touching each of these regions were skeletonised and colour
4 coded for quantification. While there were no preferential association, all contacts were
5 increased in STZ-treated (filled bars, $n = 5$) compared to control (unfilled bars, $n = 5$) retinae.
6 *D, E*: Macroglial change was assessed in control (unfilled bars, $n = 11$) and STZ-treated
7 (filled bars, $n = 11$) retinae, with no alteration in astrocyte coverage (*D*), nor Müller cell
8 gliosis (*E*) observed ($n = 6$). *F*: Kinetic analysis of VFA was used to quantify fluorescein
9 offset as a measure of BRB integrity. While arterioles and venules showed no change,
10 capillary offset was increased in STZ-treated animals (unfilled bars, control $n = 23$; filled
11 bars STZ, $n = 21$). *G, H*: The inflammatory status of microglia was assessed morphologically
12 and no difference was found in the number of monocytes / microglia in central and peripheral
13 retina (*G*, $n = 11$), cell soma size, mean process length, or the number of process branching
14 points (*H*, $n = 5$ control, $n = 8$ STZ). *I*: RNAseq data from retinal microglia taken from
15 control and STZ-treated rats were screened for genes involved in the positive (GO: 0050729)
16 and negative (GO:0050728) regulation of inflammation. While some inflammatory genes
17 were altered, key inflammatory genes were unchanged after 4 weeks of diabetes. Data
18 represented as mean \pm SEM. * $p < 0.05$. Scale bar 50 μ m.

19

20 **Figure 5. Vasoactive gene expression from retinal microglia and fractalkine-induced**
21 **vasoconstriction are altered after 4 weeks of STZ-induced diabetes.**

22 *A*: The responsiveness of retinal vessels to hyperoxic challenge was explored *in vivo* using
23 OCTA (*insets* show OCTA images from baseline and after exposure to O₂). While hyperoxic
24 challenge (filled bars) lead to constriction in the control group ($n = 10$ normoxia, $n = 6$ 100%
25 O₂), no capillary constriction was observed in the STZ cohort ($n = 12$ normoxia, $n = 7$ 100%

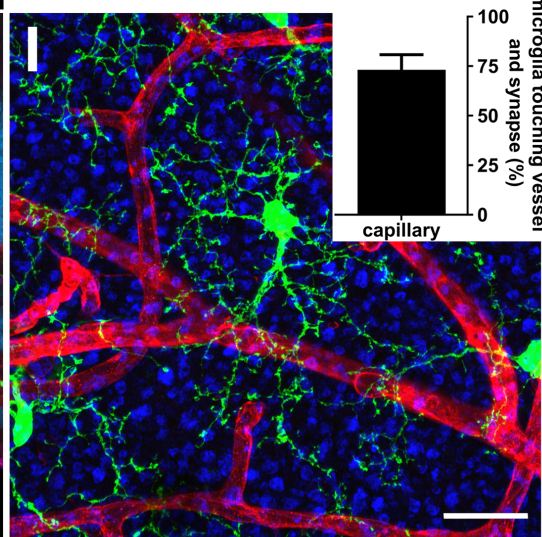
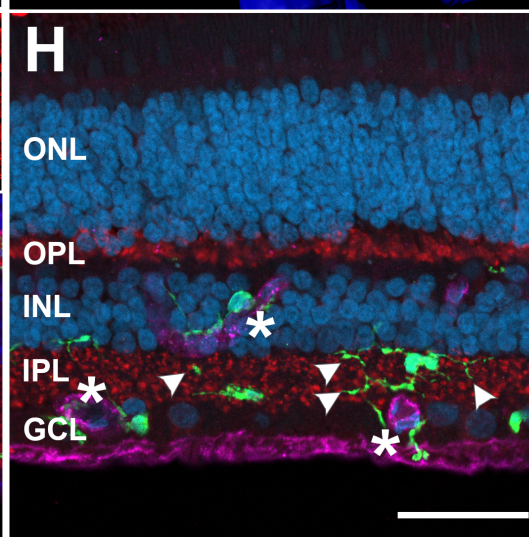
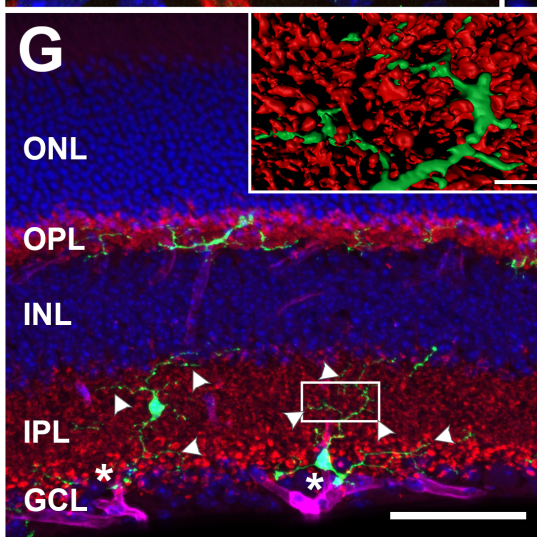
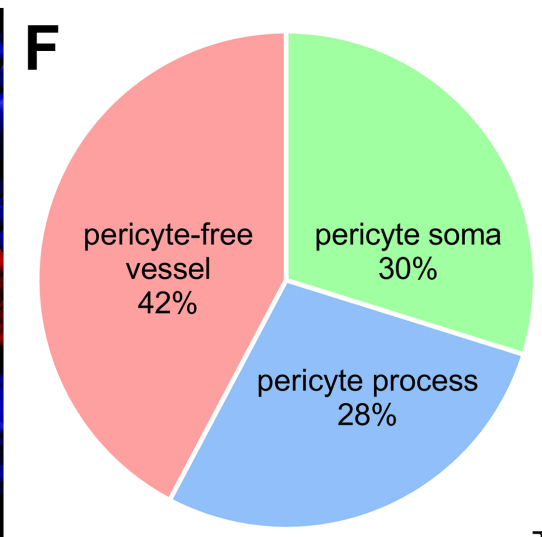
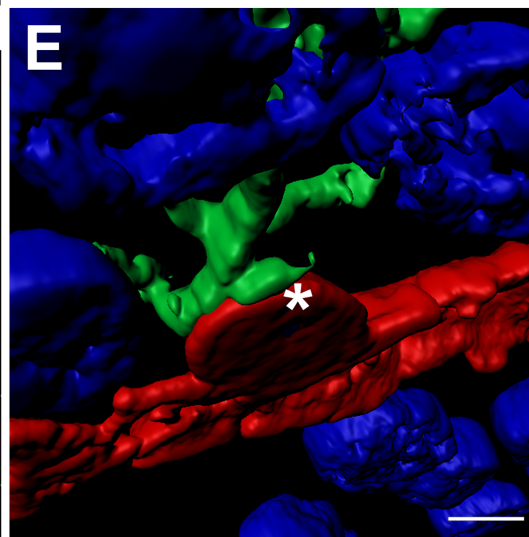
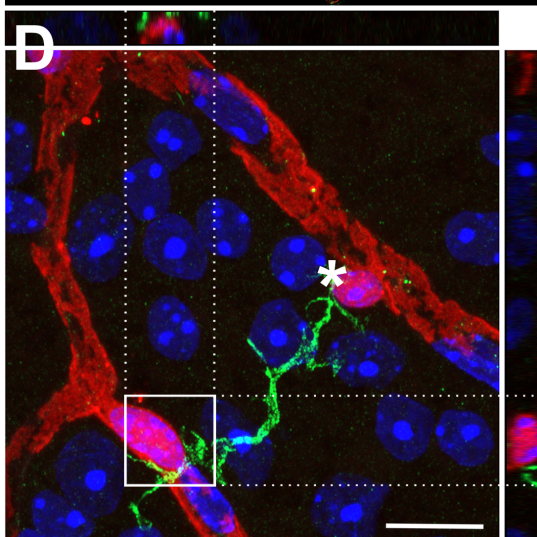
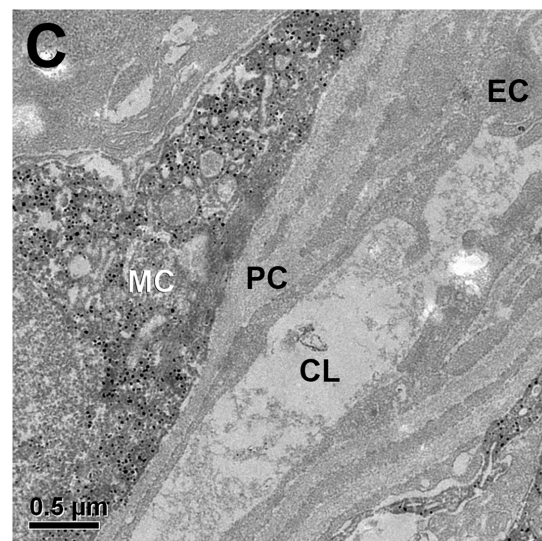
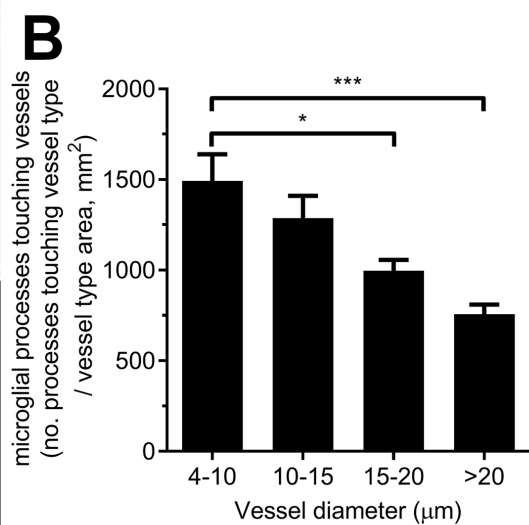
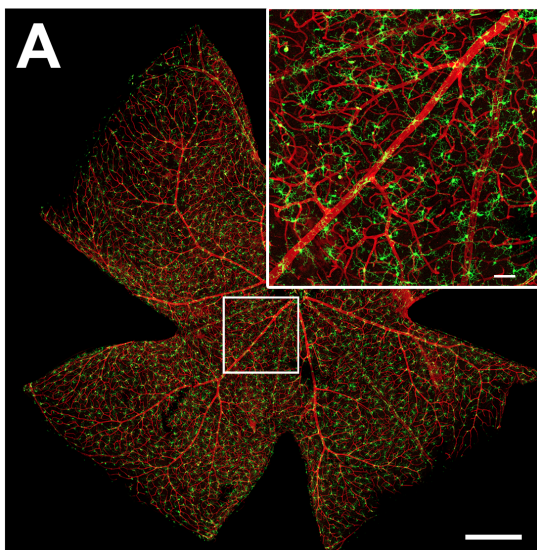
1 O₂). *B*: Microglial vasoregulation was investigated during diabetes, with 4-week STZ-treated
2 and control retinæ exposed to fractalkine *ex vivo* (representative control and STZ images in
3 *inset*). While vessels from control retinæ showed fractalkine-induced vasoconstriction (filled
4 bar), STZ retinæ exhibited no change in vessel diameter ($n = 5$ animals). *C*: Differential
5 microglial gene expression data from 4 week control and STZ-treated animals were compared
6 to vasomodulatory gene lists (vasoconstriction, GO:0097746; angiogenesis, GO:0001525;
7 vasodilation, GO:0097746), with the RAS positive regulator angiotensinogen, (*Agt*) and
8 negative regulator (*Ahr*) significantly dysregulated (FDR adjusted, citrate control $n = 5$, STZ
9 $n=4$). *D*: OCTA was used to quantify retinal superficial capillary diameter in 4-week control
10 and STZ-treated animals (unfilled and filled bars, respectively) exposed to candesartan or
11 vehicle in their drinking water. In STZ-treated animals, capillary diameter returned to
12 baseline in the candesartan-treated group ($n = 7$ control, $n = 8$, 5 STZ vehicle and
13 candesartan, respectively). *E*: Retinal blood flow was quantified using arterio-venous transit
14 time and showed increased transit time (slower blood flow) in STZ-treated animals
15 independent of candesartan treatment ($n = 8$ control, $n = 11$ and 8 STZ vehicle and
16 candesartan, respectively). *F*: Quantification of the arteriovenous ratio showed candesartan
17 treatment increased the diameter of larger vessels in STZ-treated retinæ relative to control
18 and vehicle-treated tissues ($n = 8$ control, $n = 11$ and 8 STZ vehicle and candesartan,
19 respectively). Data expressed as mean \pm SEM, * $p < 0.05$, ** $p < 0.01$, *** $p < 0.001$.

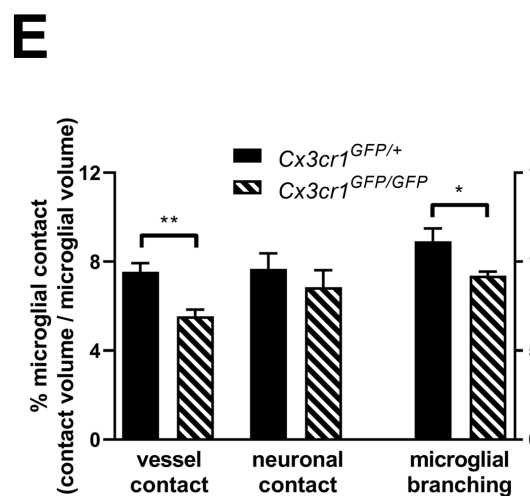
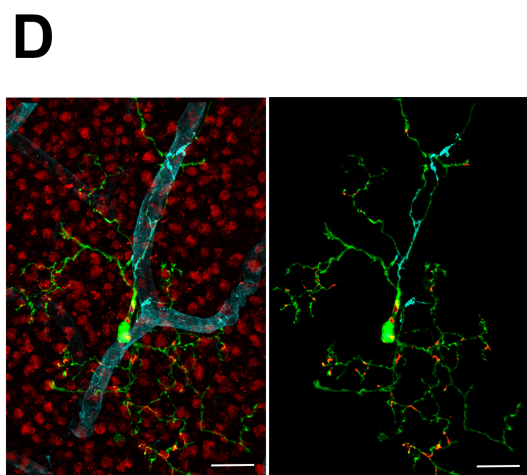
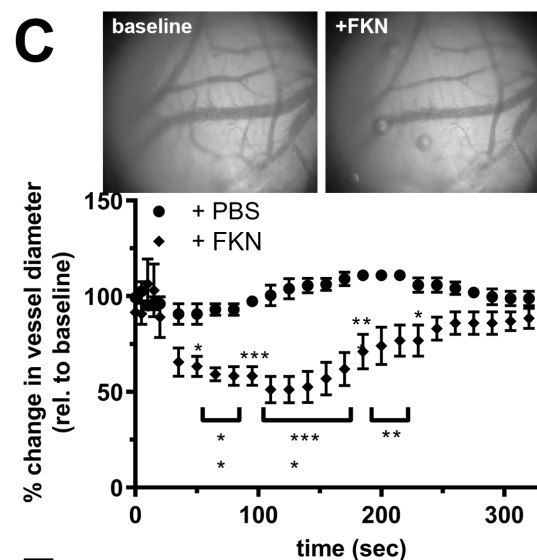
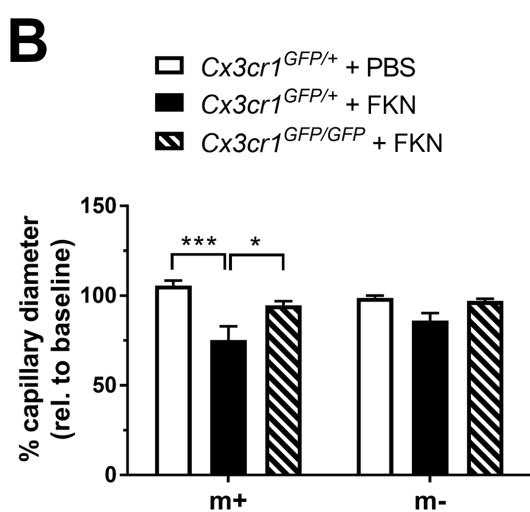
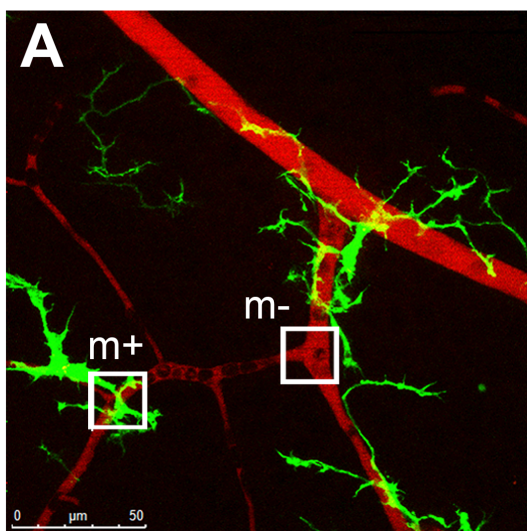
20

21 **Figure 6. Schematic representation of microglial regulation of retinal capillary**
22 **constriction.**

23 Data from this study shows microglia are structurally and functionally capable of
24 involvement in the neurovascular unit. Microglia contact neuronal synapses and retinal

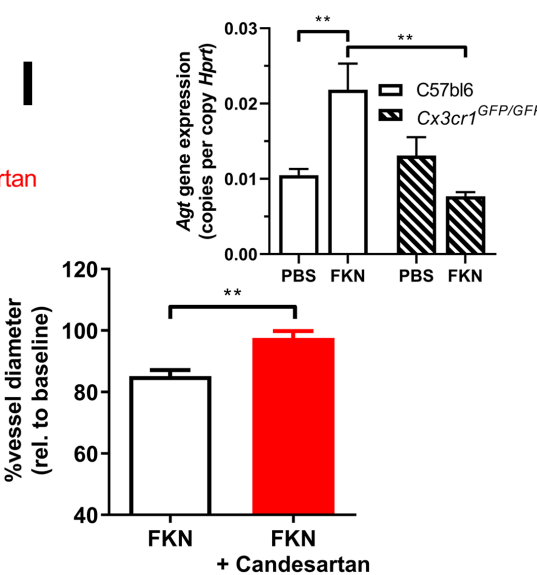
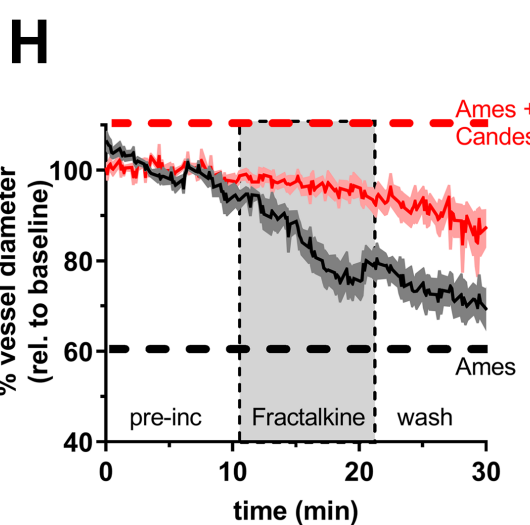
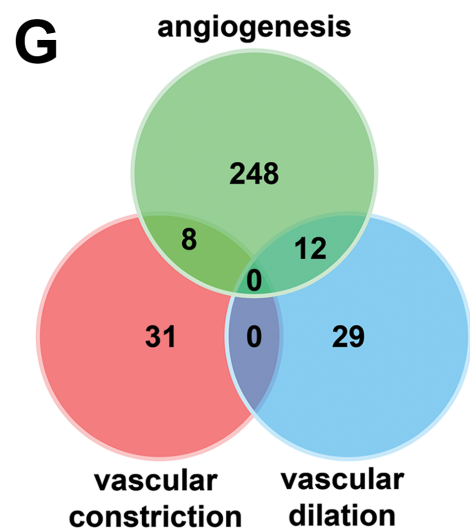
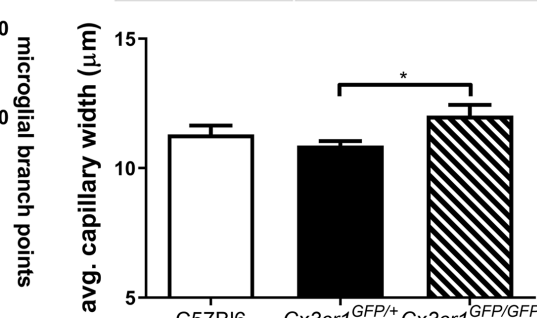
1 capillaries (including pericytes) and activation of fractalkine-Cx3cr1 signalling results in
2 capillary constriction, which is via an AT1R-dependent mechanism. Ultimately, capillary
3 regulation may occur via direct microglial mechanism or may involve contributions from
4 pericytes and / or Müller cells. FKN, fractalkine; RAS, renin angiotensin system; AT1R,
5 angiotensin II receptor type 1; PC pericyte; EC, endothelial cell.

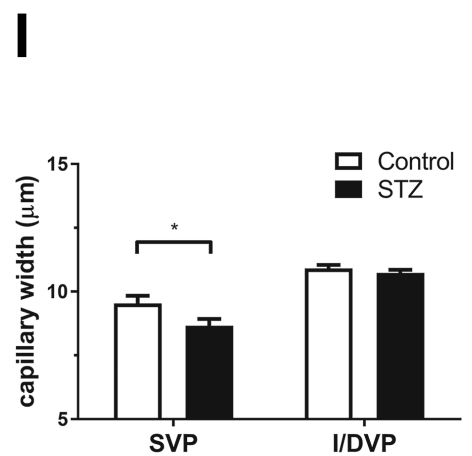
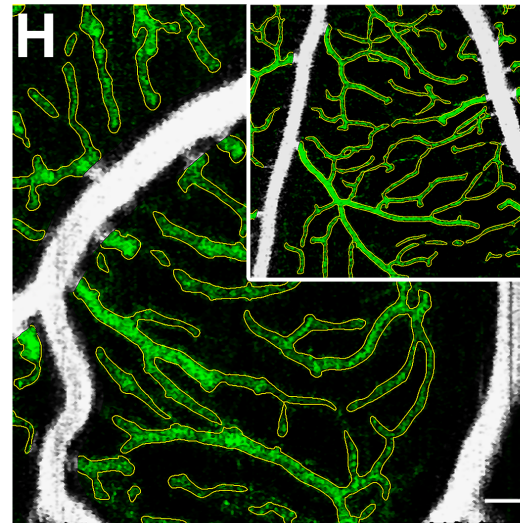
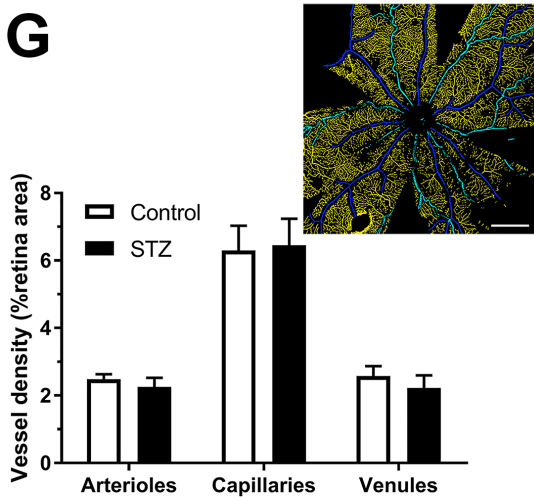
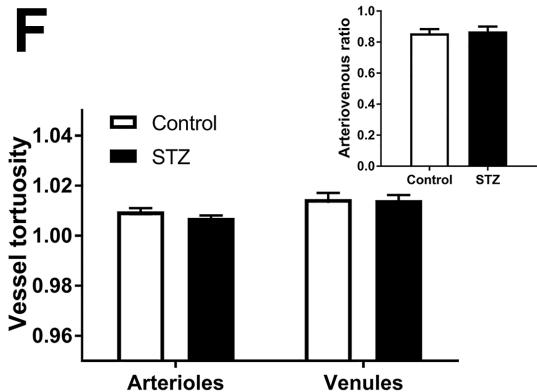
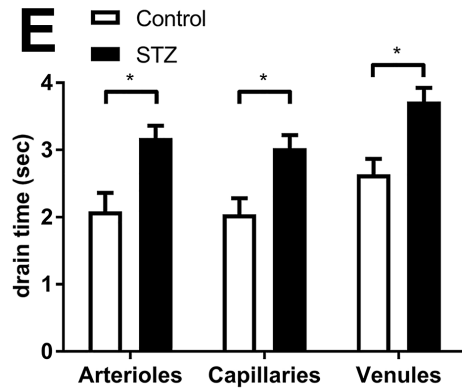
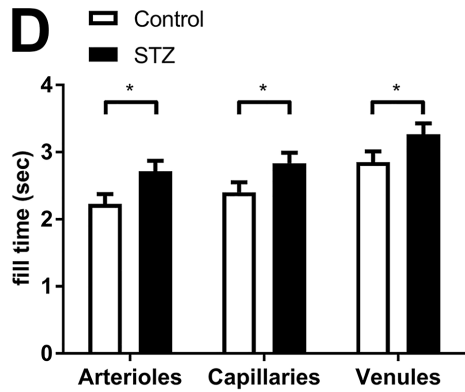
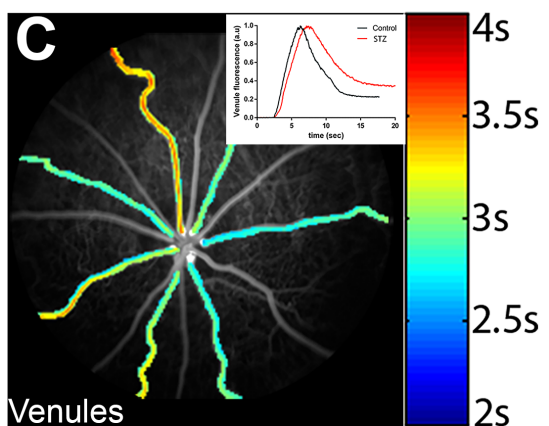
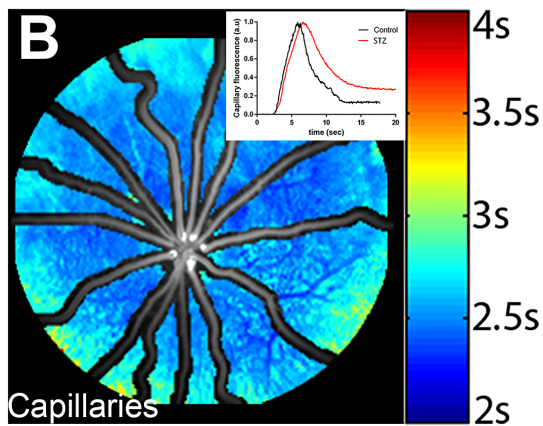
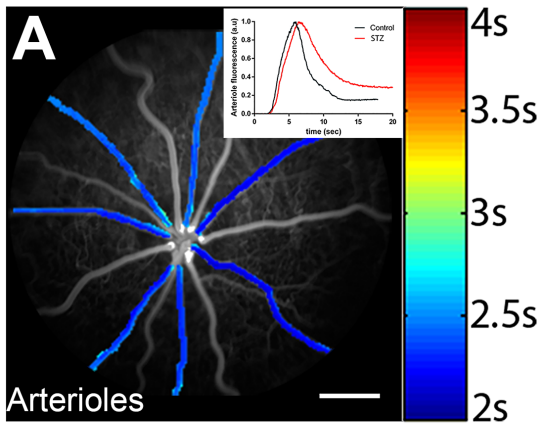


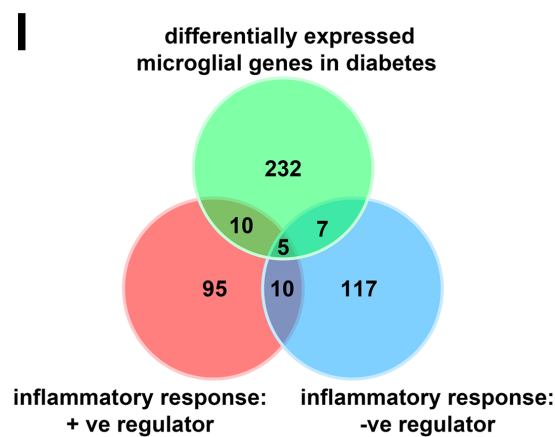
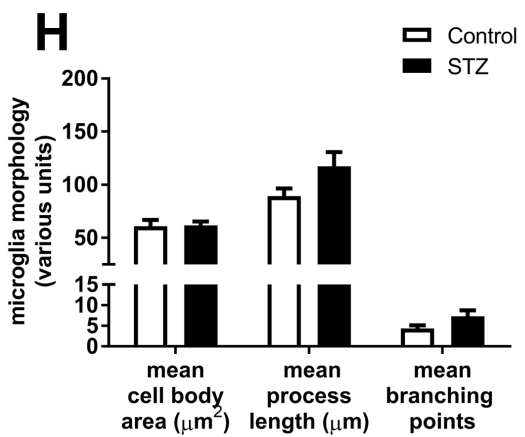
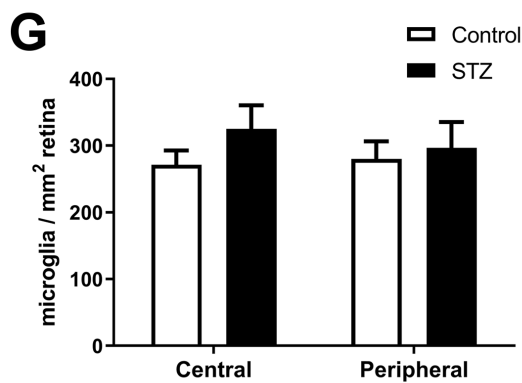
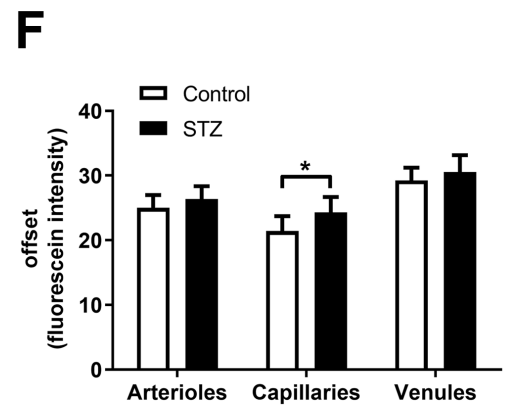
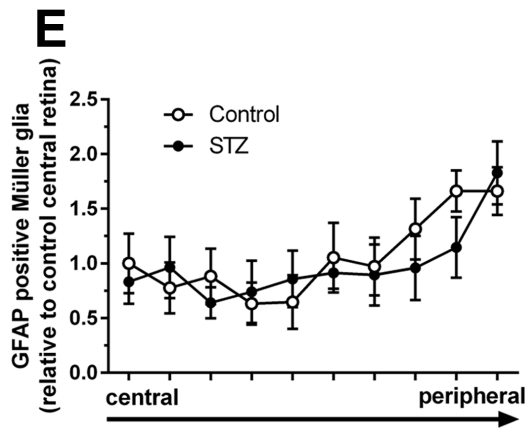
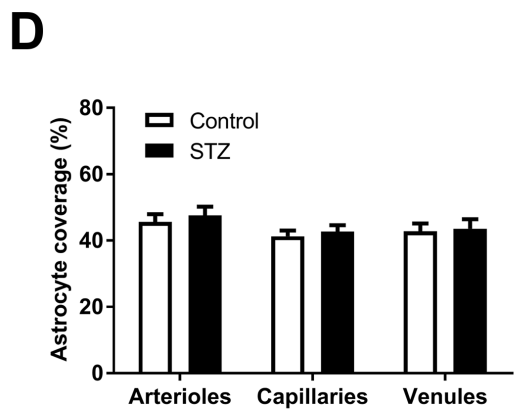
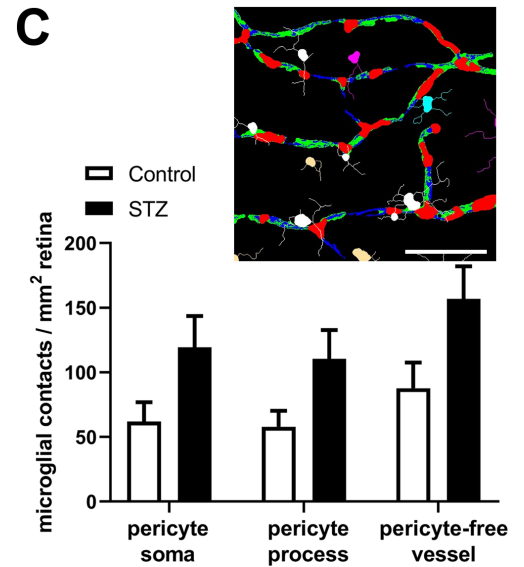
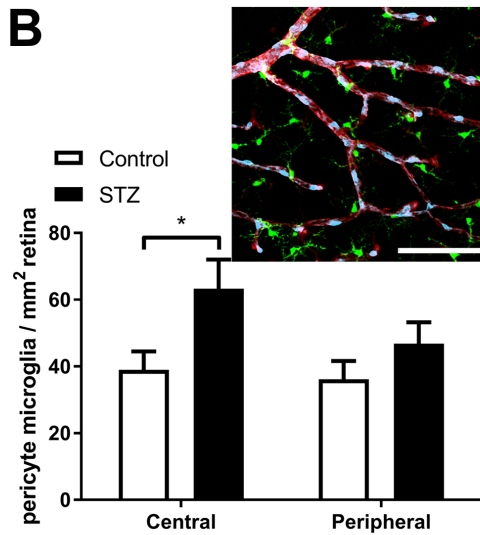
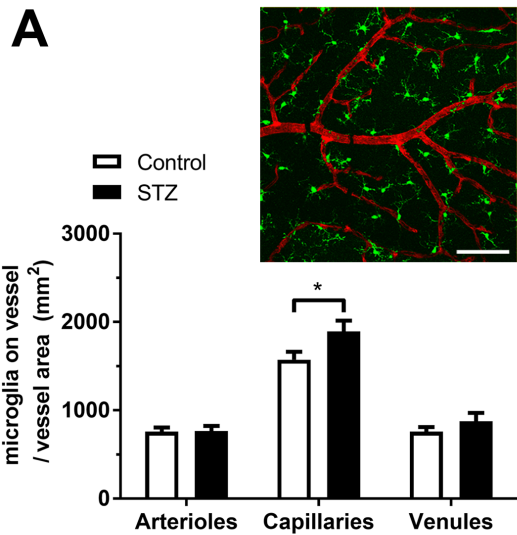


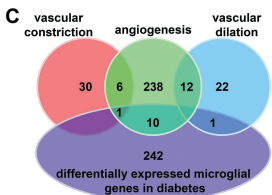
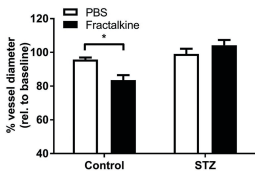
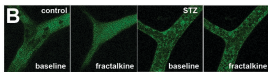
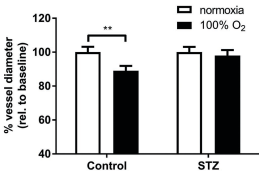
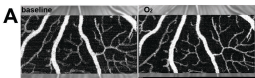
F

Genotype	Arteriovenous ratio
C57Bl6	0.96 ± 0.01
<i>Cx3cr1</i> ^{GFP/+}	0.95 ± 0.03
<i>Cx3cr1</i> ^{GFP/GFP}	0.95 ± 0.02









	gene ID	fold change	p value
+ve regulator	<i>Agt</i>	2.4	0.00007
-ve regulator	<i>Ahr</i>	3.6	0.000006

